6-1-2018

Effect of external factors on deterioration of photo voltaic panel's performance

Ahmed Osama Ghoneim

THE AMERICAN UNIVERSITY IN CAIRO

SCHOOL OF SCIENCES AND ENGINEERING

Effect of external factors on deterioration of Photovoltaic panel's performance

BY

Ahmed Osama Fahmy Ghoneim

A thesis submitted in partial fulfillment of the requirements for the degree of

Master of Science in Mechanical Engineering

Under the supervision of:

Dr. Mohamed Amr Serag El Din

Professor, department of Mechanical Engineering

The American University in Cairo

Dr. Mohamed El-Morsi

Associate professor, department of Mechanical Engineering

The American University in Cairo

May 2018

I. Abstract

Solar power is one of the most promising renewable energy resources. Thus, it has been under continuous research for improvement and enhancement. One type of solar power generators that has been appealing for the market is Photovoltaic solar cells (PVs). The performance of PV solar cells is effected by many factors. In a desert climate like Egypt, a major player in the performance is the sand or dust particles precipitation on the PV panels. This factor does not just affect the performance, but it also reflects on the utilizability of the power generation as a whole.

In the present work field measurements of the performance of 4 different sets of identical PVs inclined at different tilt angles is presented. The measurements are conducted for many different days with a wide variety of clearness index and solar intensities, at the intervals of 15 seconds. Each set includes a PV module which was cleaned daily and two which were not cleaned, thus allowing dust accumulation to build up with time. The performance of the corresponding clean and soiled modules are compared.

The study reveals that deterioration of performance of unclean (soiled) PVs is does not depend solely on the thickness of the dust layer alone, but rather by the interaction of the latter with other factors such as solar incidence angle, PV tilt angle and clearness Index.

Finally the data is used to derive best fit regressive models for both daily energy performance and instantaneous performance. The models are based on true field measurements with all variable interactions present, rather than models which investigate the effect of a single variable under controlled lab conditions as common in previous investigations.

Acknowledgements

Many people helped me along the way to get this research work done in a presentable and professional manner. My thanks and gratitude goes to my advisors, Professor Mohamed Amr Serag and associate professor Mohamed El-Morsi, I have benefited greatly from their guidance and knowledge. I have learnt much through their meetings and discussions, and I am greatly indebted to their time, patience and support. Moreover, they have given me access to all the knowledge, instrumentations and facilities needed to complete this work, and for that I am truly honored and grateful.

Also I would like to thank my family who supported me through this journey, and also the members and technicians of the mechanical department at the AUC.

I would like to thank the Egyptian National Cleaner Production Center-Ministry of Trade and Industry (ENCPC-MTI) and the Deutsche Gesellschaft für Internationale Zusammenarbeit (GIZ) GmbH Egyptian-German Private Sector Development Programme (GIZ-PSDP), for the use of the weather station provided by them.

Finally I acknowledge the American University in Cairo, which provided me with the facilities and equipment needed to complete this research.

Contents

List of figures

List of tables

Nomenclature

P_{max}	Maximum power output by PV panel	W
V_{oc}	Open circuit voltage	V
I_{sc}	Short circuit current	A
E	Daily energy output of a PV panel	Wh
I	Solar radiation intensity	W/m^2
I_d	Diffuse radiation fraction of total solar radiation	
K	Clearness Index	
G	Solar radiation on the ground	W/m^2
G_0	Extraterrestrial solar radiation	W/m^2
Θz	Zenith angle, the angle of incidence of beam radiation on a horizontal surface.	°
G_{sc}	The solar constant	W/m^2
n	day number	
φ	Latitude	$-90^\circ \leq \varphi \leq 90^\circ$
δ	Declination	$-23.45^\circ \leq \delta \leq 23.45°$
ω	Hour angle	°
γ	Surface azimuth angle	°
β	Tilt angle	°
Pclean	Power output of clean PV	W
Psoiled	Power output of soiled PV	W
Pratio	Power of soiled PV / Power of clean PV	
Eratio	Energy of soiled PV/Energy of clean PV	

Chapter one

1. Introduction

Photovoltaic solar cells generate electricity directly from sunlight. It is a source of renewable energy and is promising to become one day a main commercial source for energy generation. This is why it has been the interest of research in the past decades. PV cells convert light into electricity by utilizing semiconductor materials that absorb photons from sunlight releasing electrons that cause an electric current to flow. This phenomenon is called the photo electric effect. [1]

The continuous improvement in the performance of solar panels coupled with a continuous drop in price per kWh, is what will drive it one day to become a major power generation player. Several factors affect the performance and the efficiency of PV solar cells. To begin with, there are three different types of PV cells, monocrystalline silicon cells, multicrystalline silicon cells and amorphous silicon cells.

Monocrystalline silicon cells: pure monocrystalline silicon is what makes this type of cells. In these cells, the silicon has almost no flaws or impurities and is formed in a single continuous crystal lattice structure. The key advantage of monocrystalline cells is their high efficiency, which is usually around 15%. The disadvantage of these cells is that a complex manufacturing process is required to produce monocrystalline silicon, which results in an increase in costs. [2]

Multicrystalline silicon cells: A cheaper material is used in this type of cells, multicrystalline silicon, which overcomes the costly and high energy demanding crystal growth process. Multicrystalline cells are produced using several grains of monocrystalline silicon. In the manufacturing process, molten multicrystalline silicon is cast into ingots, then the ingots are cut into very thin wafers, after that the wafers are assembled into complete cells. The simplicity of the manufacturing process of the multicrystalline cells makes them cheaper to produce than monocrystalline cells. However, they are a little less efficient, with average efficiencies being around 12%. [2]

Amorphous silicon cells: there is a main difference between these cells and the former ones mentioned above, which is that, instead of the crystalline structure, amorphous silicon cells are made of silicon atoms in a thin homogenous layer. Moreover, amorphous silicon light absorption is more effective than that of crystalline silicon, this leads to thinner cells, this technology is also known as a thin film PV technology. The market share for the solar thin film is approximately 15%; while the other 85% is dominated by crystalline silicon. This type of cells biggest advantage is that amorphous silicon can be deposited on a wide range of substrates, both rigid and flexible. However, their disadvantage is the low efficiency, which is in the range of 6%. [2]

Other types of cells: there are other types in addition to the ones mentioned above, and they utilize a number of other promising materials, such as CdTe and copper-indium selenide (CuInSe). There is a trend today regarding the use of polymer and organic PV cells. What makes this technology appealing is that when compared to crystalline silicon technology, they potentially offer fast production at low cost, but however this new technology typically has lower efficiencies than those of the crystalline silicon technology, which is in the range of 4%. Even though, this new technology's demonstration of operational lifetimes and dark stabilities under inert conditions for thousands of hours, it still suffer from stability and degradation problems. [2]

Multiple exterior factors other than the type of the PV affect the efficiency and performance of a PV cell. Various ambient conditions can have an effect on the output of a PV power system. All These factors should be considered by the user when assessing the output of a PV power system, to get a realistic expectation of overall system output. A parameter that has big impact on the behavior of a PV system is the module temperature. It modifies the system efficiency and output energy. Also, other factors like irradiance level, ambient temperature, dirt/dust and particular installation conditions affect the performance of the PV system.

A natural characteristic of the crystalline silicon based PVs is the cell temperature. They produce higher voltage at lower temperatures and, contrariwise, to lose voltage in high temperatures. Thereby, any PV system should include adjustment for the temperature effect when assessing its performance or expected output [2]. What happens when the temperature increases, is that the band gap of the semiconductor shrinks, and the open circuit voltage (Voc) decreases. This causes the PV cells to have a negative temperature coefficient of Voc. Furthermore, a lower output power results given the same photocurrent, because the charge carriers are liberated at a lower potential [2]. Also, as the temperature increases, more incident energy is absorbed because a greater percentage of the incident light has enough energy to raise charge carriers from the valence band to the conduction band. This results in a larger photocurrent; therefore, the short circuit current (Isc) increases for a given insulation, and the PV cells have a positive temperature coefficient of Isc. This effect would raise the theoretical maximum power (Pmax) by the relationship shown by Eq. (1-1)

$$P_{max} = I_{SC} \times V_{OC} \quad \text{(1-1)[2]}$$

Solar radiation has a direct effect on the PVs power output and performance. Higher solar irradiance will give higher output. Also, other factors such as installation direction and angle of the PV will affect the amount of solar irradiance that is subjected to the PV which will affect the power output.

A major factor that will be discussed in this research, is the dust and dirt in the environment in which the PV is installed in. This factor is specific to Egypt's desert climate where the wind carries a large fraction of suspended particles, and where rain is very seldom and hence the accumulated particles are not naturally washed away. These dust particles when accumulated on the PVs will alter its performance considerably, and this would be discussed thoroughly in the next chapters.

Chapter 2

2.1 Literature review

A limited amount of investigations addressed the negative effects of dust accumulation on PVs. The reason for this is probably because of the difficulty to come up with a meaningful quantitative results and due to this being a problem specific to desert climates. Different papers take into account different parameters, and take different methodologies in their experiments.

The accumulation of dirt on the front surface of PV modules is what is referred to as the soiling phenomena, and is an important factor for a PV system's performance. This is especially in locations that have scarcity in rain, or dry conditions and even frequent dust or sand storms. Thereby, the power loss due to soiling is a function of the type and thickness of dust layer, the latter is affected by the strength of the wind, the weight of the suspended particles in the wind and the length of time since the last rainfall and cleaning schedule [3].

The soiling effect increase when the period between successive rainfalls increases, and this can be noticed in warm climates such as the one in Cyprus. This is more evident during the summer period. In areas of frequent rainfall, it is demonstrated that the rain could clean the PV modules to an extent of restoring the performance to within 1 % of full power [3].

Studies explore several factors that affect or influence soiling. For example, one study examined the physical properties of the dust itself and its effect on the PV cell. El-Shobokshy and Hussein [4] in their experiments simulated the dust with limestone, cement and carbon particulates. They used halogen lamps as their source of light simulating the sun. While keeping the light intensity constant i.e. solar intensity constant and varying the different densities of dust, the test was repeated several times. The study revealed that the cement particles had the greatest impact on the performance, with a 73 g/m^2 deposition of cement dust resulting in an 80% drop in PV short-circuit voltage; while atmospheric dust with mean diameter 80 µm reduced the short circuit current by 82% at 250 g/m^2. Fine carbon particulates about 5 µm were found to have the most deteriorating effect on the PV efficiency. The study also found that finer particles have a greater impact on PV performance than coarser particles, as shown in Figure(2-1), for the same dust type. [4]

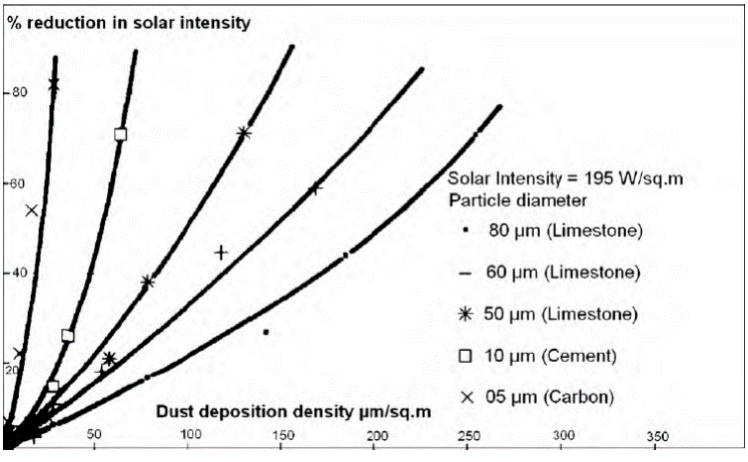

Fig. 2-1 Solar-intensity reduction in response to dust deposition [4]

Another study with the same approach aimed to study the effect of different pollutants on a multi-crystalline photovoltaic module [5]. In this study the pollutants used were; red soil, carbonaceous fly-ash, sand, calcium carbonate and silica, all were spread with depositions of 5 and 10 g/m^2. This paper concluded that the highest reduction in voltage was due to fly-ash as Figure (2-2) shows;

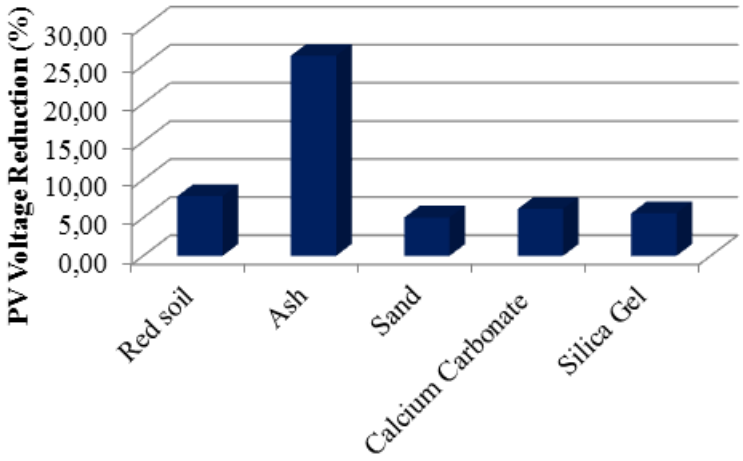

--

Fig. 2-2 Reduction in PV voltage due to different pollutants [5]

Goossens et al. [6] designed an experiment to study the impact of wind velocity and orientation characteristics of PV system on soiling. Simulations based in a wind tunnel were used in this investigation, along with, experimental field investigations in the Negev Desert for various wind systems and system orientation. As seen in figure (2-3), their PV system was inclined at 45° with mirrors on east and west. The simulation study for the wind sector (SW 10°W–N 10°E), showed a general increase in dust accumulation under all wind directions, with increase in wind speed. However, the deposition of dust decreased as the elevation from the ground increased with increased wind speeds. A notable observation was the high dust accumulation in the afternoon and evening for strong westerly winds. While southwesterly winds caused high dust accumulation in the evenings alone. Also, for the southwesterly winds, little difference was noticed in dust deposition between noon and afternoon. Table 1 summarize the noticeable observations. It is noticed that the impact of dust storms is that by day the largest amount of dust settled on the PV panels, while by night, the largest amount of dust settled on the eastern mirrors. [6]

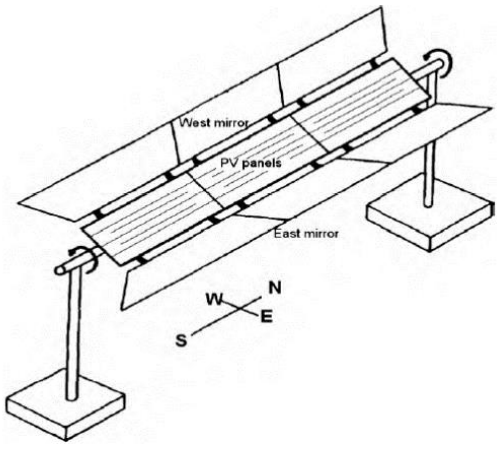

Fig. 2- 3 Experimental PV setup investigating dust deposition under various wind[6]

Table 2-1 summary of observations on dust deposition for various wind directions

Summary: salient observations on dust deposition for various wind directions

Wind direction	Dust deposition trend		
	Minimum	Maximum	Progressive decrease/increase
North	Morning	Noon	Decrease during evening
North-west	Mid morning	Noon	Decrease during afternoon
West	Forenoon (for high velocity winds)	Afternoon	Decrease during evening
South-west	Morning	Afternoon	Decrease during evening

Another experiment done by Mamadow and Goosens [7] determined the efficiency of sediment sampler with a wind tunnel. The sediment sampler was designed to measure the accumulation of Aeolian dust. In their investigation a Frisbee sampler and a marble dust collector was used. Efficiency was established for five different velocities and eight grain sizes, velocities ranging from 1 to 5 meters/second, and grain sizes from 10 to 89 μm.

In a more difficult experiment to investigate the effect of the dust accumulation on glass transmittance, Hegazy [8] conducted an experiment that lasted for one year, for the subtropical climatic region of Minia in central Egypt. The experiment apparatus consisted of nine square glass plates, each plate was 3 mm thick and had an exposed surface area of 0.09 m^2. The procedure was that one plate was kept clean as the reference plate, while the others were mounted on flat wooden frames facing south and having different inclinations (0°, 10°, 20°, 30°, 40°, 50°, 60° and 90°) to study the extent of dust collection over a month. A formula relating the dust deposition ω in g/m^2 to the glass transmittance reduction ($1 - \tau/\tau_{clean}$) was deduced by following a nonlinear regression on the experimental data, the deduced formula is shown in Eq. (0-1);

$$\frac{1-\tau}{\tau_{clean}}(\%) = 34.37\,\mathrm{erf}(0.17\omega^{0.8473}) \qquad \text{(0-1)[8]}$$

Where,

$erf^{-1}(x)$ is the Gauss error function.

$(1 - \tau/\tau_{clean})$ is glass transmittance reduction

ω is the dust deposition in g/m^2

The investigation also concluded that for tilt angles less than 30° the dust deposition is largely site climate specific, and therefore the decrease in transmittance is also climate specific. The accuracy of the empirical correlation developed was in the range of ±6%. Also, it allowed for the calculation of the transmittance reduction in glass transmittance for at a certain tilt angle and exposure time to the atmosphere. Results from this study could be effectively used along the belts of the Atlantic Ocean to the Persian Gulf for smaller tilt angles, with a recommendation of a weekly cleaning cycle for places exposed to moderate dust levels and an immediate cleaning after a sand storm. [8]

Another experimental investigation was conducted by Eliminir et al. [9] in Cairo, Egypt at the National Research Institute of Astronomy and Geophysics. This experiment consisted of a 100 glass plates with different tilt and azimuth angles. Over the period of seven months the glass transmittance was evaluated at regular intervals, for the predominant wind conditions, including thunderstorms. The study concluded that a reduction in dust deposition from 15.84 g/m^2 at tilt angle of 0° to 4.48 g/m^2 at a tilt angle of 90°

caused a corresponding increase in transmittance from 12.33% to 52.54%. A governing equation between the dust deposition and reduction in transmittance was also derived. Another conclusion was that differences in humidity led to the formation of dew on the PV's surface which coagulated dust. Weekly cleaning cycle was recommended for moderately dusty places. [9]

Another study divides the effect of dust into two categories. The first is dust accumulation which is the accumulation of sand particles on horizontal glass surface is found to exponentially reduce the available area for transmission of incident photons. The second category is dust pollutant which is air pollution causing degradation of PV performance as a result to accumulation of solid particles varying in type, composition and shape. [10] The main difference between the two is one studies the effect of dust naturally occurring in for example desert climate, the other examines the effects of pollutant such as byproducts of combustion in the air. Following the first classification of dust accumulation, Neil [11] used analytical and numerical models to represent dust depositions on PV panel in dry climate areas, and supported by a laboratory investigation of sand particles accumulation on a glass surface. The sand particles accumulation on horizontal glass surface was found to decrease the available area for photon transmittance to produce the curve shown in figure (2-4);

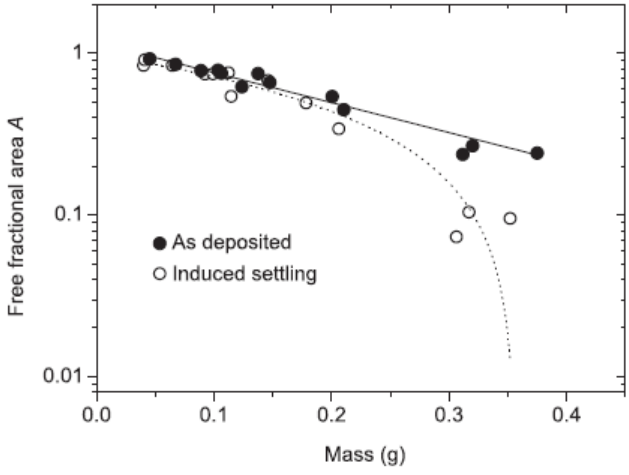

Fig.2 -4 Reduction in the free fractional area of a glass slide with increasing quantities of sand [11]

Filled circles show the as-deposited coverage while open circles show coverage after application of gentle disturbance to the glass slide. The solid and dotted lines are exponential and linear fits to the data, respectively. Following the other classification of dust as a pollutant, Kaldellis and Fragos [12] experimented on the energy difference between two identical PVs, one being clean and one being artificially polluted with ash. Ash was chosen since it was a typical pollutant from incomplete hydrocarbons' combustion mainly originating from thermal power stations and vehicular exhausts. This research produced the curve shown in Figure (2-5);

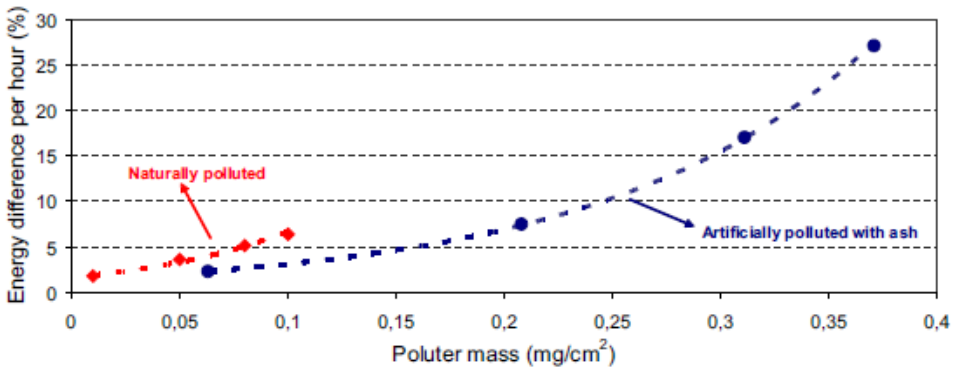

Fig. 2-5 Energy difference between clean and the polluted pair panel for various mass deposition in cases of naturally and artificially polluted PV [12]

Several factors impact dust accumulation and also impact performance. For example, tilt angle as mentioned before. Sayigh et al [13] investigated the dust deposition on a tilted glass plate located in Kuwait City. Their experiment concluded that the dust was found to reduce the transmittance of the plate from 64% to 17% for tilt angles ranging from 0° to 60°, respectively, after 38 days of exposure to the environment. Another factor would be humidity; humidity can affect the irradiance level of sunlight reaching the PV plates through water vapor particles, as shown in Figure(2-6)Another effect would be humidity ingression to the solar cell enclosure. [13]

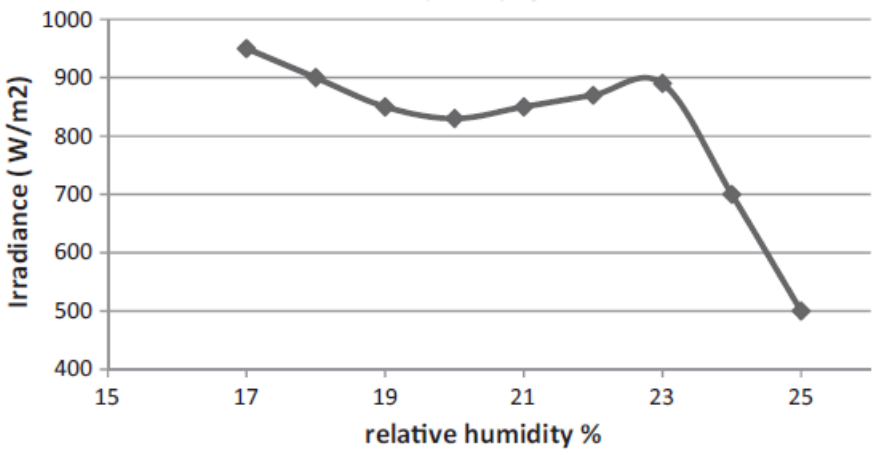

Fig. 2-6 Variation of irradiance level with relative humidity [13]

Another research work (Ibrahim et al., 2009) [3] compared between three PVs in Egypt, one was cleaned every two months, and another was not cleaned at all for a whole year and a third one that was kept clean. The energy production results showed that the one-year dusty module produced 35 % less energy while the two-month dusty module produced 25 % less energy compared to the clean module. Figure 2-7) shows the soiling accumulation after a period of one year for the systems installed in Egypt. [3]

Figure 2-7 Soiling accumulation after a period of one year for the systems installed in Egypt [3]

Another experiment [15] that was carried out in Egypt as well, investigated the effect of dust on the three modules during complete year and was focused on the dusty days for the period between January and June of 2015. The experiments were performed in Heliopolis University, Cairo-Egypt, where the dusty days have been recorded manually with observing the data of the ambient temperature, module temperature and the output power for the system. This experiment results are summarized in Table 2-.

Table 2-2 Experimental results of power output [15]

Date	Wind Speed (m/s)	Average Daily Power Yield per Month	Power Yield on the Dusty Day	Power Yield One Day After
06 January, 2015	11 m/s (normal 4.1)	15.82	16.75	5.32
10 February, 2015	10 m/s (normal 5.1)	16.57	15.41	6.10
18 February, 2015	11 m/s (normal 5.1)	16.57	14.80	2.53
08 March, 2015	11 m/s (normal 5.7)	16.57	18.74	11.02
26 March, 2015	09 m/s (normal 5.7)	21.00	21.87	14.15
31 March, 2015	09 m/s (normal 5.7)	21.00	22.25	19.70
10 April, 2015	10 m/s (normal 4.6)	22.93	19.01	8.49
28 April, 2015	10 m/s (normal 4.6)	22.93	23.04	22.09
13 May, 2015	10 m/s (normal 4.6)	21.92	20.13	18.41
27 May, 2015	8.8 m/s (normal 4.5)	21.92	14.82	13.5
27 June, 2015	7.7 m/s (normal 4.7)	21.59	21.30	20.28
09 September, 2015	5.0 m/s	20.44	9.50	17.90

The study concluded that dusty days cause layers of dust to settle on the PVs, which have a significant impact on the power output with output drops up to 49%, and this happened even with the various, modern PV panel technologies utilized in the study. [15]

In the current research, an experiment is designed and constructed to test the effect of dust on the performance of PV panels for four different tilt angels, as the tilt angle affects the dust accumulation on each PV. Moreover, the effect of dust on the performance for various clearness indices and solar incidence angles is investigated. Then the performance of the PVs is linked on how it affects the utilizbility of the PVs.

The basis of the concept of utilizability is that if only radiation is above a critical intensity, then it is useful radiation. This threshold or critical intensity is the intensity required to give enough power to operate or generate a specific power requirement. The value of critical radiation, $\mathrm{I_{Tc}}$ is the value of incident radiation on the collector plate that is just as equal as the energy losses in the plate.

If the incident radiation on the collector surface, $\mathrm{I_T}$, is equal to $\mathrm{I_{Tc}}$ all of the absorbed energy will be lost and there will be no useful gain. If the incident radiation exceeds $\mathrm{I_{tc}}$ there will be useful gain and then operation is recommended. From that concept the utilizability of any hour in the day, $\mathrm{Ø_h}$, is the fraction of that hour's total energy that is above the critical level [14]

$$\mathrm{Ø_h} = \frac{(\mathrm{I_T} - \mathrm{I_{Tc}})}{\mathrm{I_T}} \qquad \text{(0-2) [14]}$$

In operation the utilizibality of a single hour is not significant what is considered is the utilizibity of this hour over the course of a month. For example, utilizability for a particular hour (say 10 -11 a.m.) of a month (say January) of N days (say 31), in which the hour's average radiation is $\bar{\mathrm{I}}_T$ is useful:

$$\phi = \frac{1}{N}\sum_{1}^{N}\frac{(\mathrm{I_T} - \mathrm{I_{Tc}})}{\bar{\mathrm{I}}_T} \qquad \text{(0-3)[14]}$$

1. The month's utilizable energy *for the hour* is then (N $\bar{I}_T$ ϕ)
2. Summing up the results for all hours (10-11, 11-12...) for the month, gives the month's utilizable energy.

2.2 Research objective

The objective of the present study is to investigate the effect of various external factors on the performance of PV modules exposed to actual desert type environmental conditions. This includes the effect of naturally accumulated dust and its interaction with other factors, such as solar beam incidence angle, and clearness index.

Having established the basic parameters that affect the output from the PV modules, regression analysis will be conducted to derive relations that relate the effect of the different parameters on both the instantaneous performance of the PV module and their total daily output. These relations may be used to make more reliable estimates of performance degradation under real field conditions. They can also be employed to make informed decisions regarding the optimum frequency of cleaning, and other uses.

Chapter 3

3. Experiment procedure and Test rig

A tests rig is designed and constructed to investigate the effect of dust accumulation on PVs' performance subjected to natural site conditions at different tilt angles. To study the effect of dust accumulation on the PV panels, and how this effect interact with other variables. This experiment differs from previous work by taking into account the compounded effect of different external factors on the performance of PV panels, rather than performing a controlled experiment in the lab.

The test rig consists of 12 PV solar panels, each three will be mounted at a different angle. Four different angles will be used, those angels are 15, 30, 45 and 60 degrees. This would examine the effect of the tilt angle of the PV on the performance deterioration, due to dust accumulation and other factors. The performance deterioration is expected to be influenced mainly by the thickness and type of dust deposition, thickness being strongly affected by the tilt angle. The dust type at the experiment site is composed mainly of sand grains, as the site is at the American University in Cairo new campus closely resembles an open desert environment, thus ashes, cement, etc. are notably absent.

The solar panels used are 12 identical panels of the model Philadelphia solar ps-m72h-300, it is a Polycrystalline (multicrystalline) cell and it has a short circuit current of 8.51 Amps and an open circuit voltage of 44.77 Volts. Its maximum power output is rated at 300 W under standard testing conditions. Table 3-1 summarizes the PV's specifications

Table 3-1 PV panel's specifications

Type	Panel Dimension (H/W/D)	weight	V_{oc}	I_{sc}	Connector Type
Polycrystalline	1965x990x40 mm	25.5 kg	44.77 V	8.51 A	MC4

A weather station is used to monitor wind speed, humidity, ambient temperature and solar radiation. It is supplied from THEODOR FRIEDRICHS and Co, shown in Figure 3-1) to Figure . The weather station is composed of a wind speed sensor, a wind direction sensor, a pyranometer for measuring global solar radiation and a humidity and temperature sensors. The humidity sensor measuring range is 0 - 100 % calibration accuracy of ±1.5 %. The wind speed sensor range is 0 – 41 m/s with accuracy of ± 0.3 m/s. The pyranometer measuring range is up to 2000 W/m^2 with an error less than ±20 W/m^2.

.

Figure 3-1 Pyranometer for measuring solar radiation

Figure 3-2 Humidity sensor

Figure 3-3 Wind speed sensor, wind direction sensor

Two data loggers are used to collect the information needed, one collects the output current and voltage from each PV panel, and the other collects the weather station data. The panels are connected to the data logger, shown in Figure (3-4), and to a load, the load is basically a coil heater of 7 ohms resistance, shown in Figure . The data logger records a reading every 15 seconds, the left screen display is the current/10 amps, and the right screen displays volts, and it has two memory SD cards to save that data. The PVs are installed facing south. The site latitude angle is 30°. The current and volt readings are to an accuracy of ± 0.01 A and ± 0.1 V. As shown in Figure (3-4), all the 7 Ohm coil heaters are stacked in one stand manufactured specifically for the experiment. Also, it has a top pyramid shape to protect the connections and the heaters from rain.

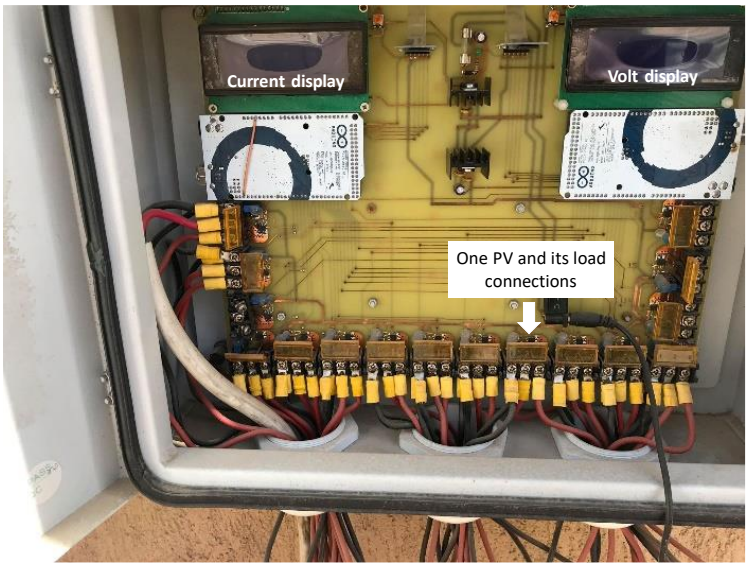

Figure 3-4 PVs data logger with all PVs and Loads connected

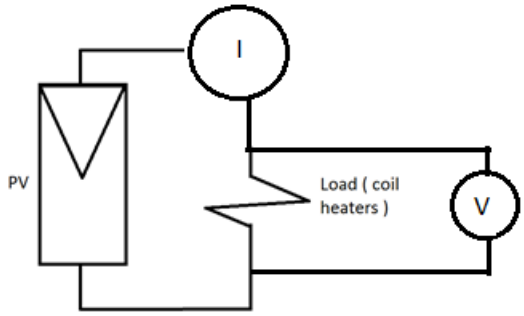

Figure 3-5 Circuit connection between the PV, data Logger and the load

Figure 3-6 Rack and housing of coil heater loads, each load connected to its terminal in the logger and to a PV

Figure 3-7 Angle 60 PVs with the left PV cleaned every day

3.1 Experimental procedure

The experiment proceeds as follows; for every tilt angle there are three panels, one is cleaned regularly, the other two are not cleaned at all. The power and energy output average is taken for the soiled PVs, in this case two PVs are soiled for each angle to reduce error and avoid biased results. The output power is calculated from the current and voltage readings taken from the PVs' data logger. Then the performance, power and energy outputs of the PVs are compared and interpreted on how cleaning and tilt angle affects them, and in return the effect of these factors on utilizability is estimated. Also, the impact of various clearness indices and incidence angles is examined on the dusted PVs.

The clean PVs are denoted by the letter "A" followed by their tilt angle, thereby the clean PV at 60° would be A60 and the one at 45° would be A45 and so on. B and C would denote the soiled PVs. The average of the two soiled PVs is denoted by AV and then its angle, so the average of B45 and C45 is AV-45 and so on.

The experiments ran for three months, starting on October 3rd 2017 till January 4th 2018. The cleaned PVs were cleaned daily, in the early morning to avoid the PVs being hot, and the data was collected from the data logger. During the same period weather data was collected from the weather station data logger.

For the first two days all PVs were kept clean to examine their performance and then examining the soiling effect. All the PVs were cleaned on the mornings of October 3rd and October 4th. After this, only one PV from each rack was cleaned daily. The following is a step by step explanation for the procedure:

1. The test rig was constructed and the PVs are mounted on 4 different racks, each rack at a tilt angle
2. The connections were made between each PV and its load and the data logger, 4 mm^2 copper wires were used for all connections.
3. The weather station was installed on the test site, and connected to its data logger, to record solar intensity.
4. The weather station data logger took data every 60 seconds.
5. All 12 PVs are cleaned to initiate the experiments.
6. The experiments started on the October 3rd 2017and all the PVs were cleaned on October 3rd and October 4th
7. Starting from the October 5th of onwards, only PV A, from each rack, was cleaned daily. As explained earlier letter A denotes the clean PV from each rack.
8. Data was collected all the way up to January 4th2018.

9. The current and volt measurement for each PV were recorded by the logger every 15 seconds, and stored as an excel sheet on the memory cards on the PVs data logger. From those readings the power and daily energy was calculated. Also, Power-Time curve was produced daily for each PV.
10. The total daily energy was calculated, as it is the area under the Power-Time curve
11. Power and energy values of soiled PVs were compared to those of the clean PVs, for each rack.
12. Also, the impact of different clearness indices on the soiled PVs' performance was examined.
13. The impact of solar radiation angle of incidence was also investigated.
14. Finally, linking all these factors to the compound effect they have on performance
15. Studying the effect of performance deterioration on utilizability
16. Correlation of measured data to get regression models that represent the power and energy deterioration over time.

3.2 Error analysis

As stated earlier the error in the current and voltage readings is ±0.01 A and ±0.1 V, respectively. The uncertainty in the power calculation is calculated from the fractional error as Eq. (3-2) states [16]. If

$$q = \mathrm{x}\,\mathrm{z} \tag{3-1}$$

Then error in q is

$$\frac{\delta q}{|q|} = \sqrt{\left(\frac{\delta x}{x}\right)^2 + \left(\frac{\delta z}{z}\right)^2} \tag{3-2}$$

Hence, the uncertainty in the power calculation is estimated as shown by Eq. (3-3);

$$Error\ in\ power = power \times \sqrt{\left(\frac{0.1}{volt\ reading}\right)^2 + \left(\frac{0.01}{current\ reaidng}\right)^2} \tag{3-3}$$

The associated error in the energy calculations is then calculated by summing all the power errors squared under the square root, as shown in Eq. (3-4).

$$Energy\ error = \sqrt{\sum power\ errors^2} \tag{3-4}$$

Based on this, the uncertainty in the energy calculation is estimated to be $\pm 2.1\%$. A sample is shown in Figure (3-8).

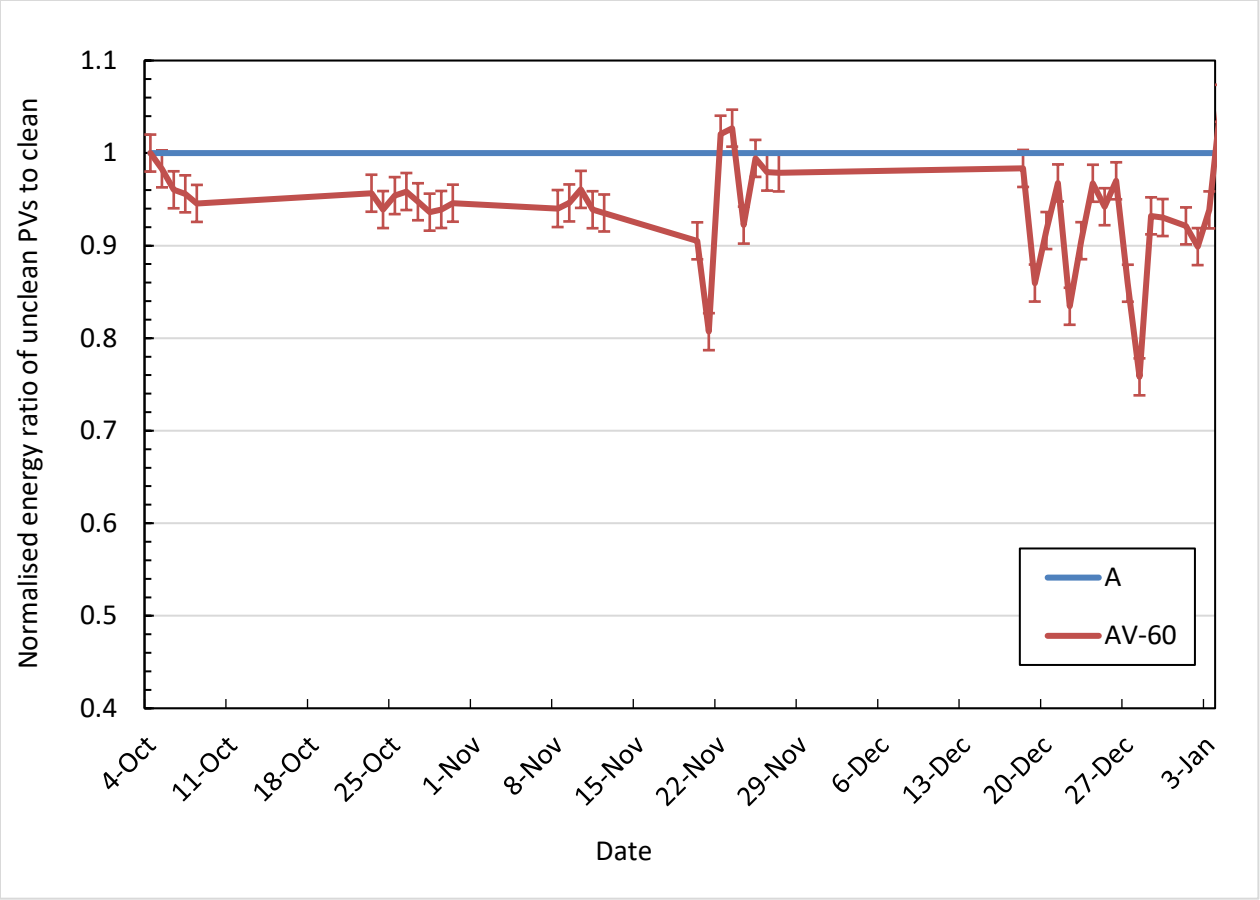

Figure3-8 Energy ratio with error bars for PVs inclined at 60°, A is the clean PV and AV-60 is the average energy ratio of the soiled B60 and C60

Chapter 4

4. Results and Discussion

There are 12 PV panels to be examined, each three at the same angle. There are 4 angles in the experiment, 60°, 45°, 30° and 15° each angle with three PV panels.

All PVs were kept clean for the first two days; 3rdand4th of October 2017, then one on each rack was cleaned daily. Fig. (4-1) displays the power output over 5 days, from the 3rd of October till the 7th of October for PVs A60, B60 and C60. Fig. (4-2) shows the power time curves over the same period for the 45 degrees tilt angle PVs; A45, B45 and C45. The same is for Fig. (4-3) showing Power time for 30 tilt angle PVs and Fig. (4.4) for the 15 tilt angle PVs. All were kept clean the first two days and then only PV A from each rack was cleaned daily.

As seen in Fig. (4-1) all PVs started out producing very close output, but in the last day where A60 was the only clean panel, it had a slightly higher power output.

Over the same period the power output of the PVs on 45 degrees were recorded. And as seen in Fig. (4-2), A45 shows a slightly higher output at the last day when the other two have not been cleaned anymore.

For the first two days when all PVs were kept clean they produced almost identical power output, but after that when only A45 was kept clean it started to produce a slightly higher output. Overall all PVs at angle 45 produced a higher power output than those at angle 60 for those same 5 days.

For lower angles dust accumulate at a higher rate effecting the power output drastically as seen on the fig (4-3).

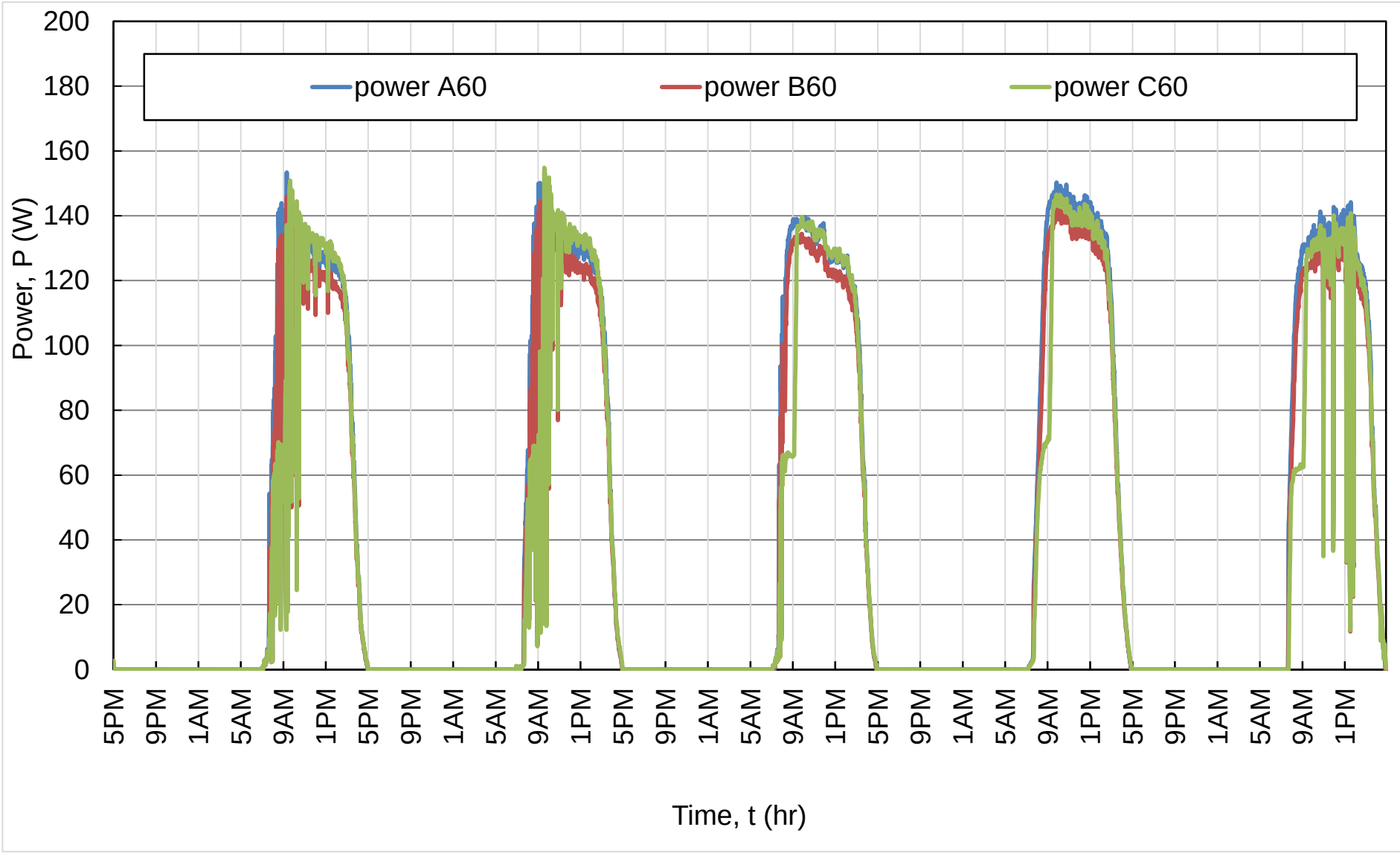

Figure 4-1 Power –time of 'A60', 'B60' & 'C60' for 5 days from 3rd of October till 7th of October, where all were kept clean for the first two days, and then only A 60 was cleaned

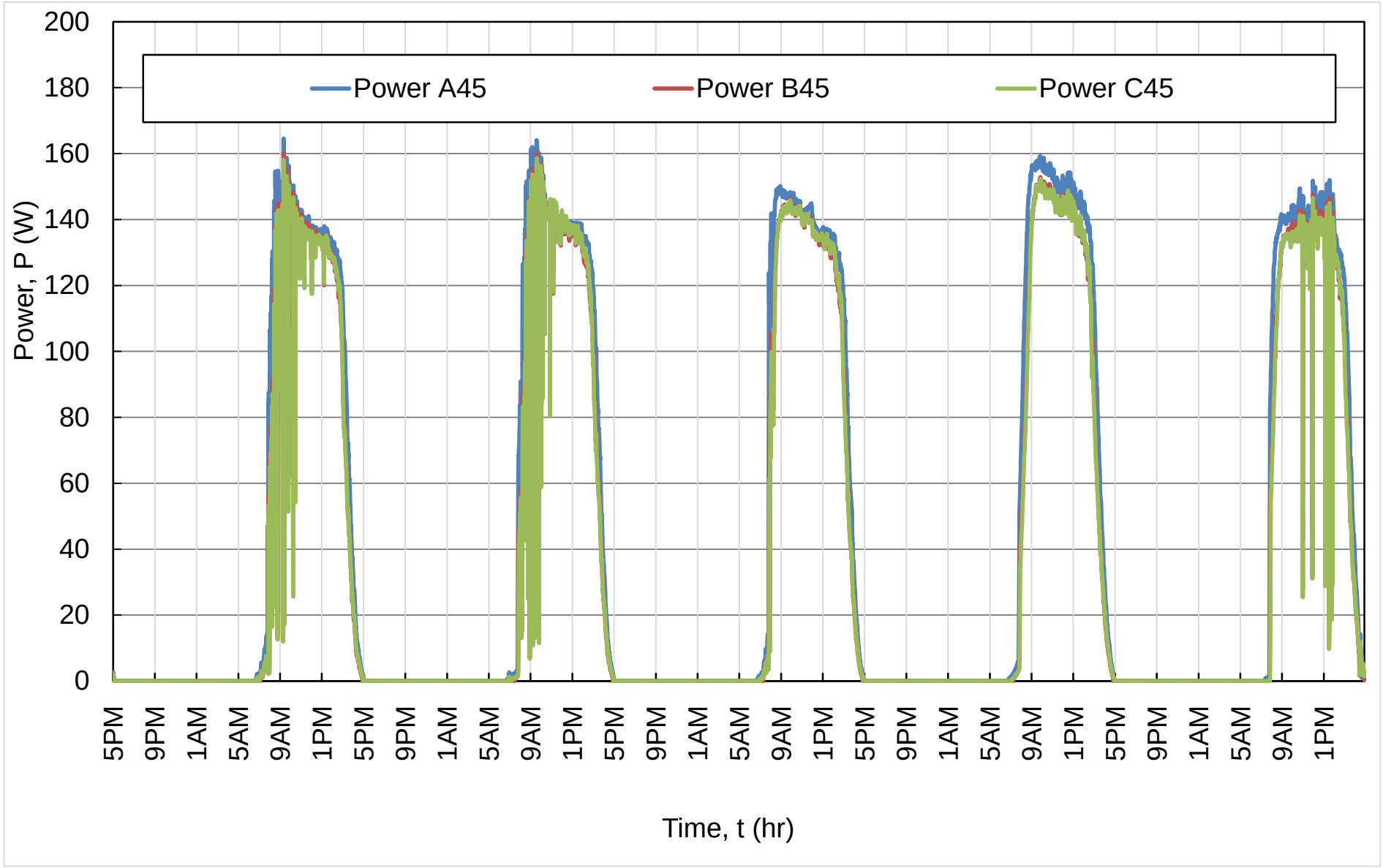

Figure 4-2 Power time output of PVs A45, B45 & C45 From 3rd of October till 7th of October

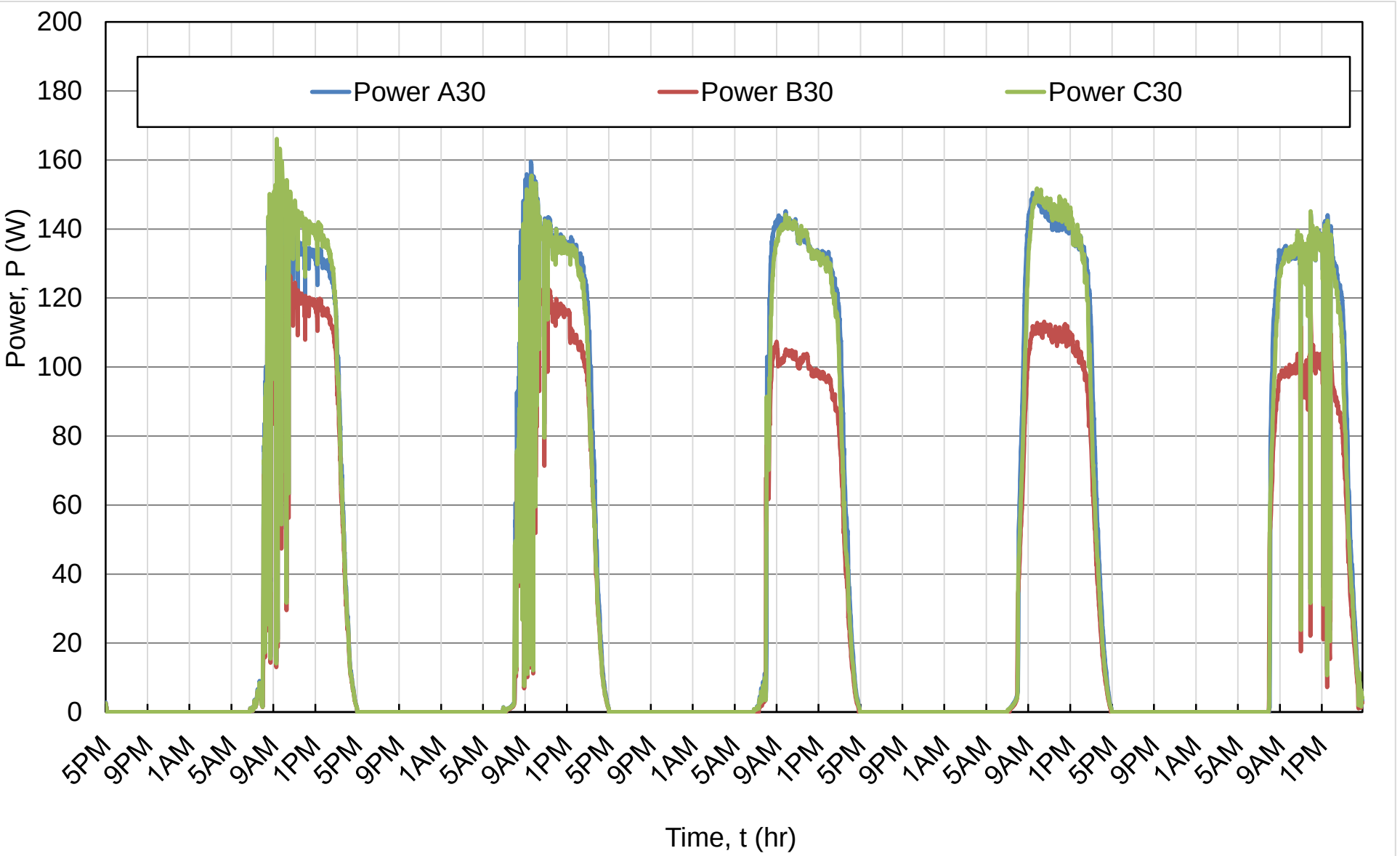

Figure 4-3 Power time output of 'A30', 'B30' & 'C30' at angle 30 for 5 days

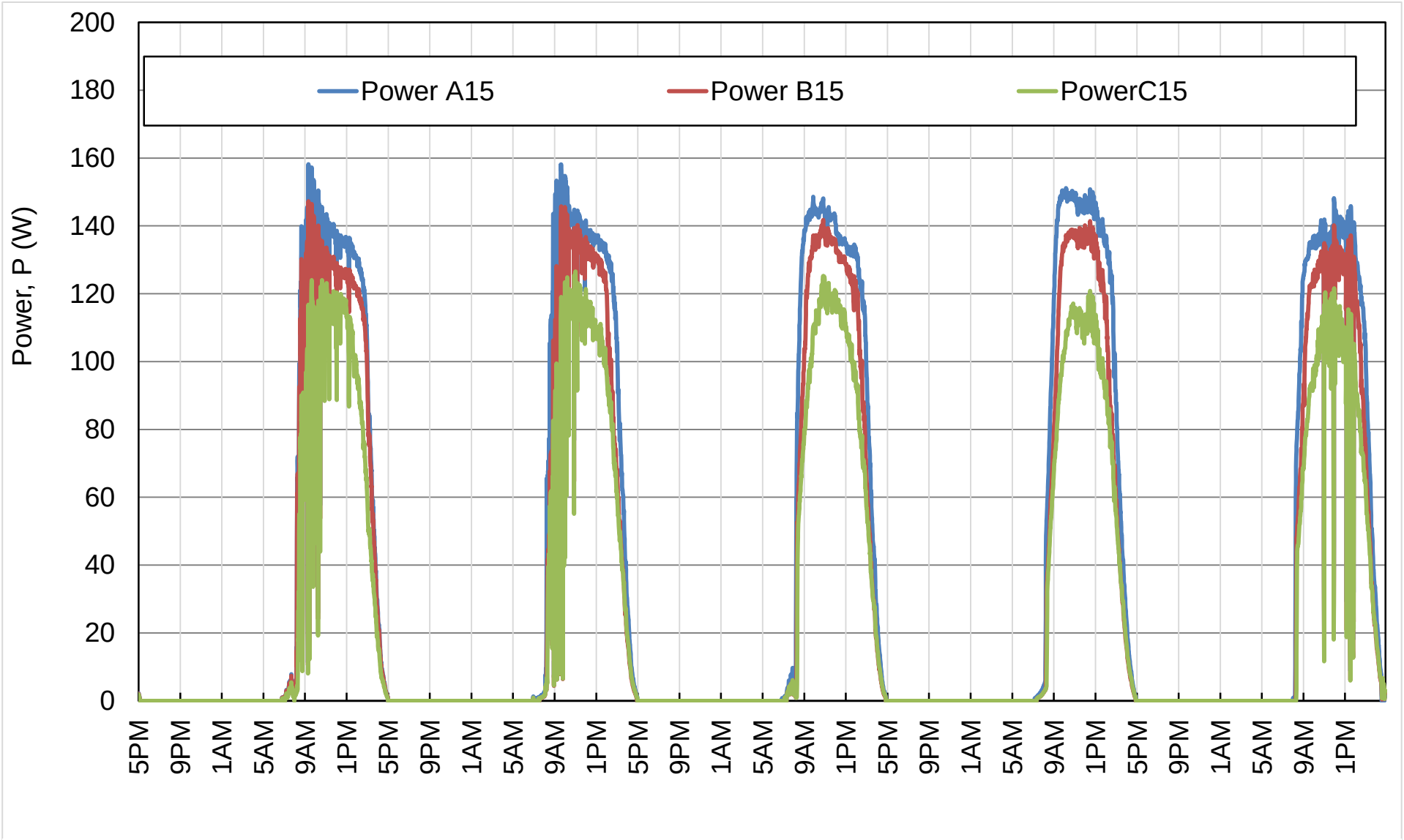

Figure 4-4 power-time output for angle 15, A15 (clean), B15 & C15 for the same period

Fig-(4-5) and Fig (4-6) shows the first day power time curve and the last day power-time curves.

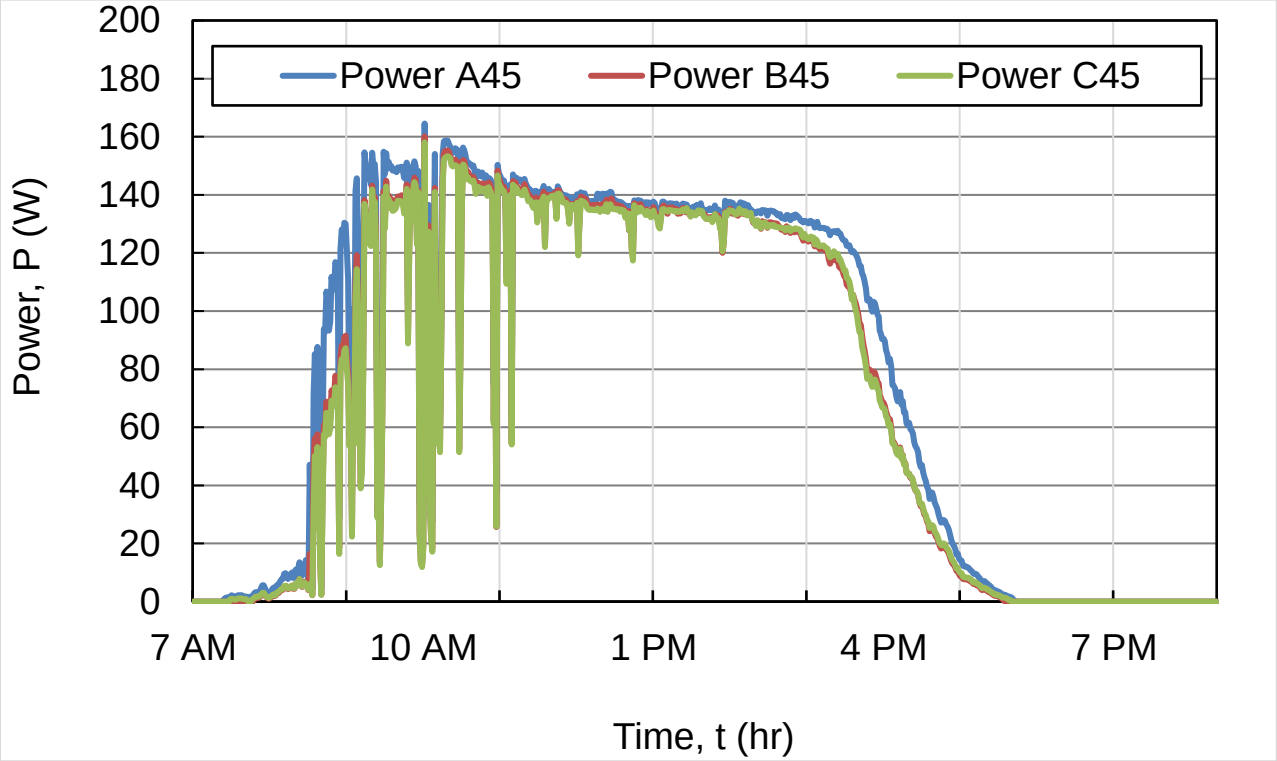

Figure 4-5 Power time curve for A45, B45andC45 on the 3rd of October when all PVs were clean

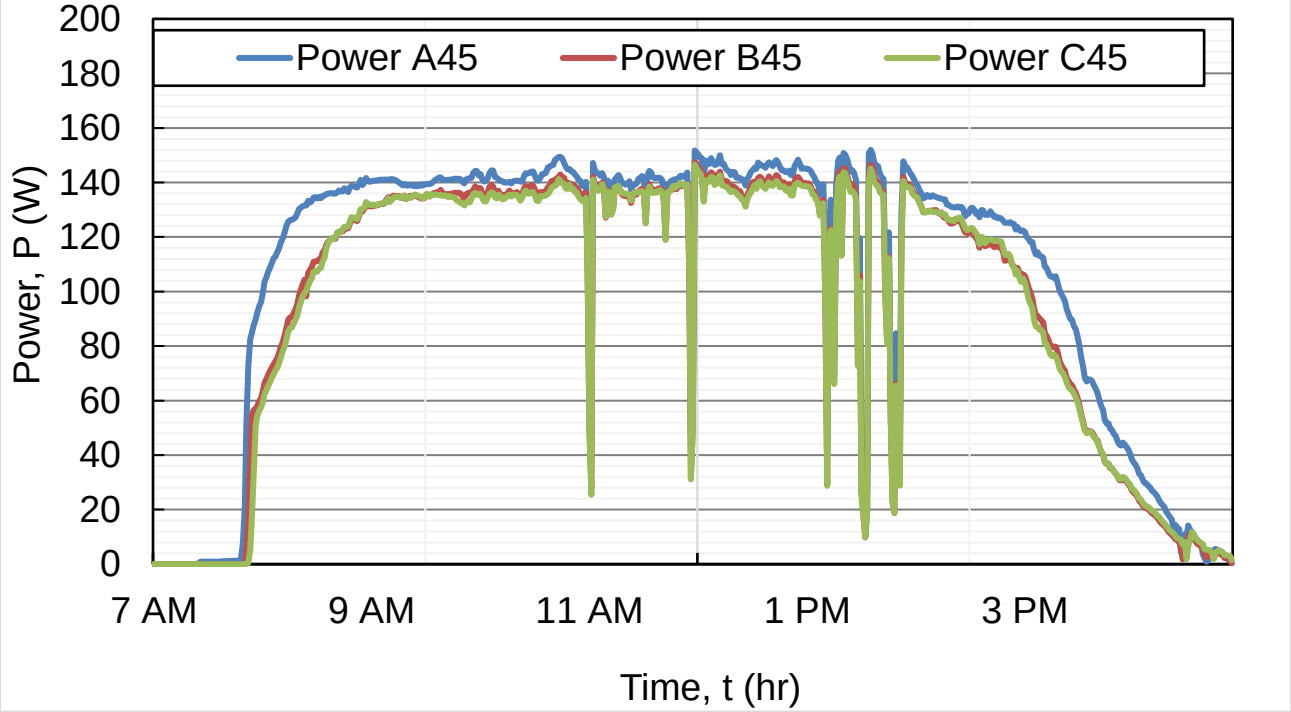

Figure 4-6 power time curve for A45, B45andc45 on the 7th of October when only A45 was clean

It is noticed that the power output by the soiled PVs decreased at the beginning and the end of the day, this is due to the fact that lower angle of incidence by the sunlight occur at those times. The solar radiation over those five days were recorded by the weather station and the following diagram (Figure 4-7) shows how it varied in Watts/m^2.

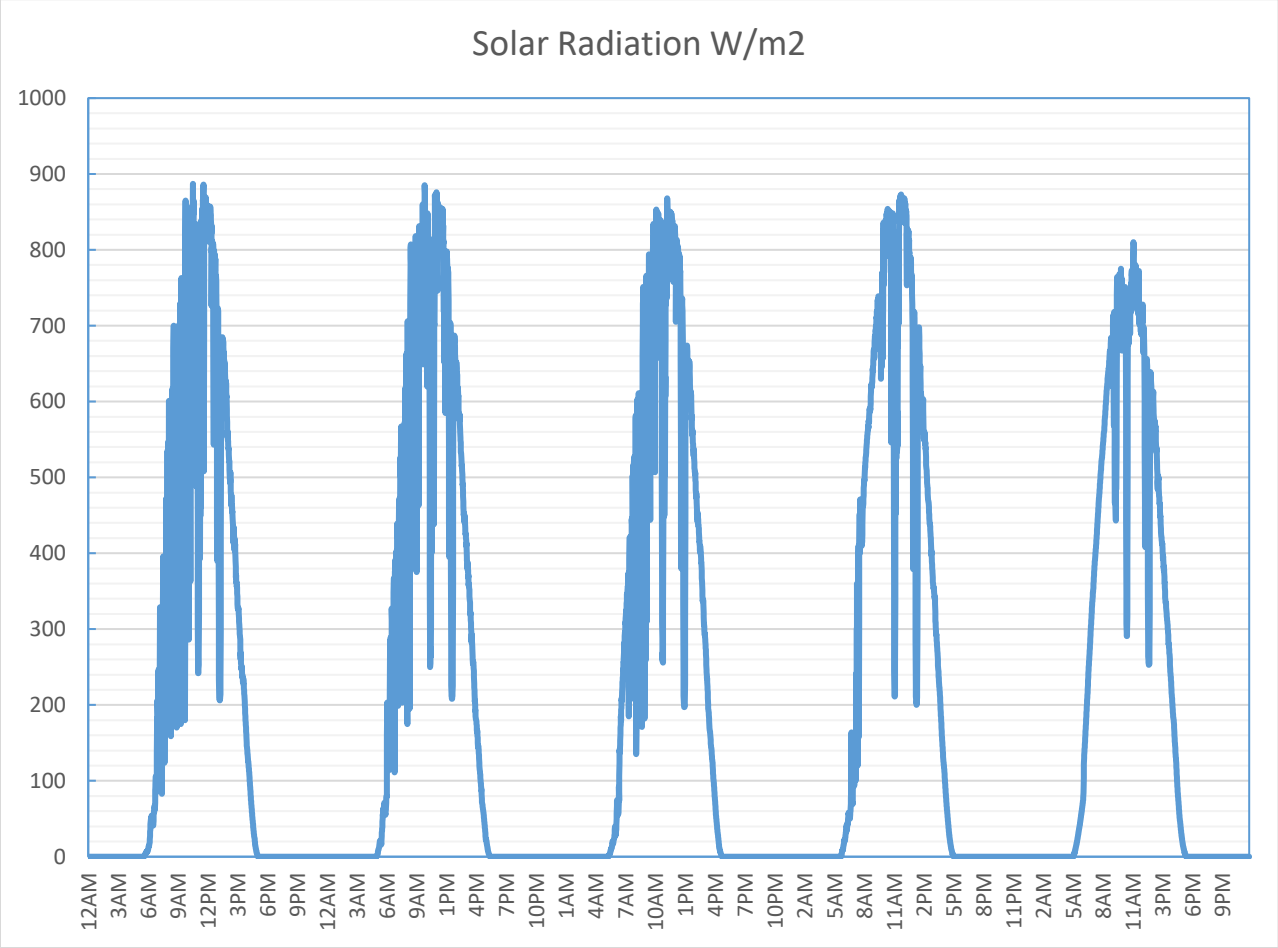

Figure 4-7 Solar radiation recorded by the weather station over the examined 5 days

The radiation on the last day decreased slightly which explains why all PVs had a slighter lower power output. The following figure shows all PVs power outputs against solar radiation.

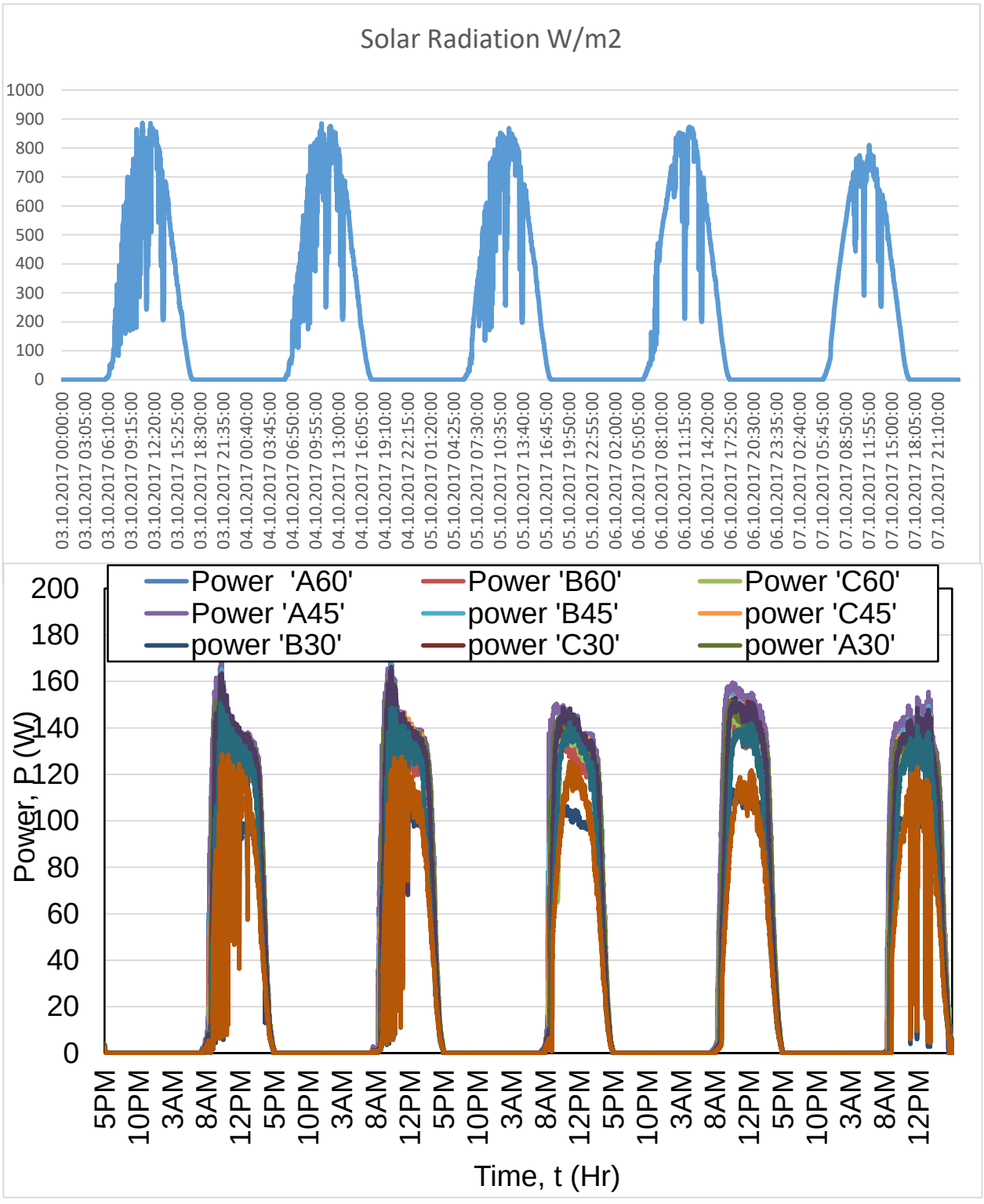

Figure 4-8 all PVs power outputs against solar radiation

All PVs on all four tilt angles showed the same behavior of very close output in the beginning but at the last day the clean (A) PV of each angle had a slightly higher output.

The power was recorded keeping one PV clean on each angle (PV A) all the way up to the 4th of January. The total energy was calculated from the power time curve to compare total energies of each PV for each day.

To compare how the total energy output of each PV varied from the 4th of October till the 4th of January, total energy ratio of the soiled PVs to the clean PV was plotted. Even though they did not all produce the exact same energy at day 1 when all were clean, but the curve starts from one for all PVs as a correction factor is used to normalize these data so they would all start from zero. Some Panels produced more energy than the others when all were clean and that was taken into account when calculating the ratios. Figures, (4-9), (4-10), (4-11) & (4-12) show the energy ratio curves from 4th of October till the 4th of Jan.

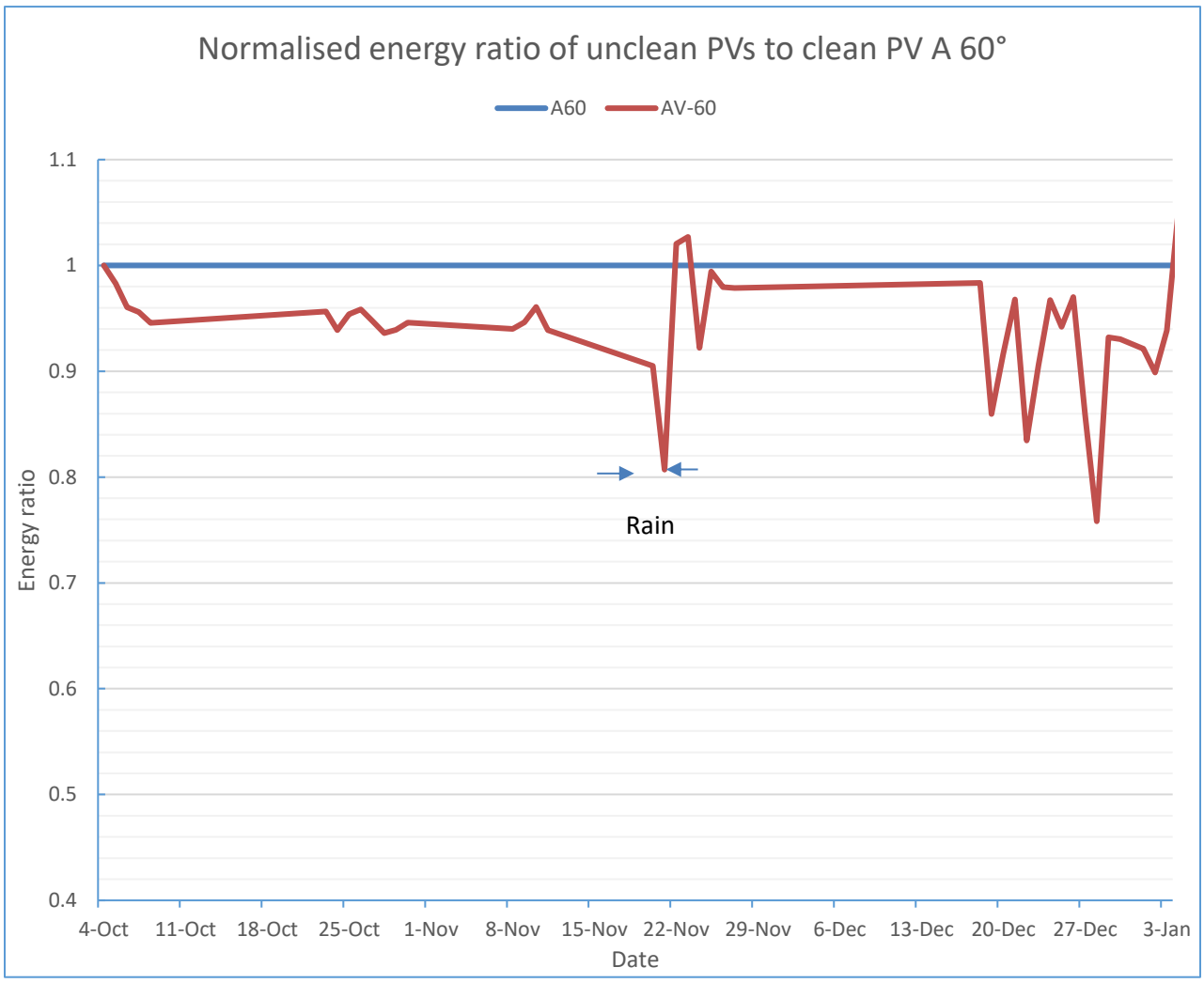

Figure 4-9 Angle 60 PVs energy ratios of soiled PVs (AV60) to clean PV A

The decrease in energy ratio is higher as the angle gets less steep, so it is notices in the angle 45 the ratio decrease Is bigger.

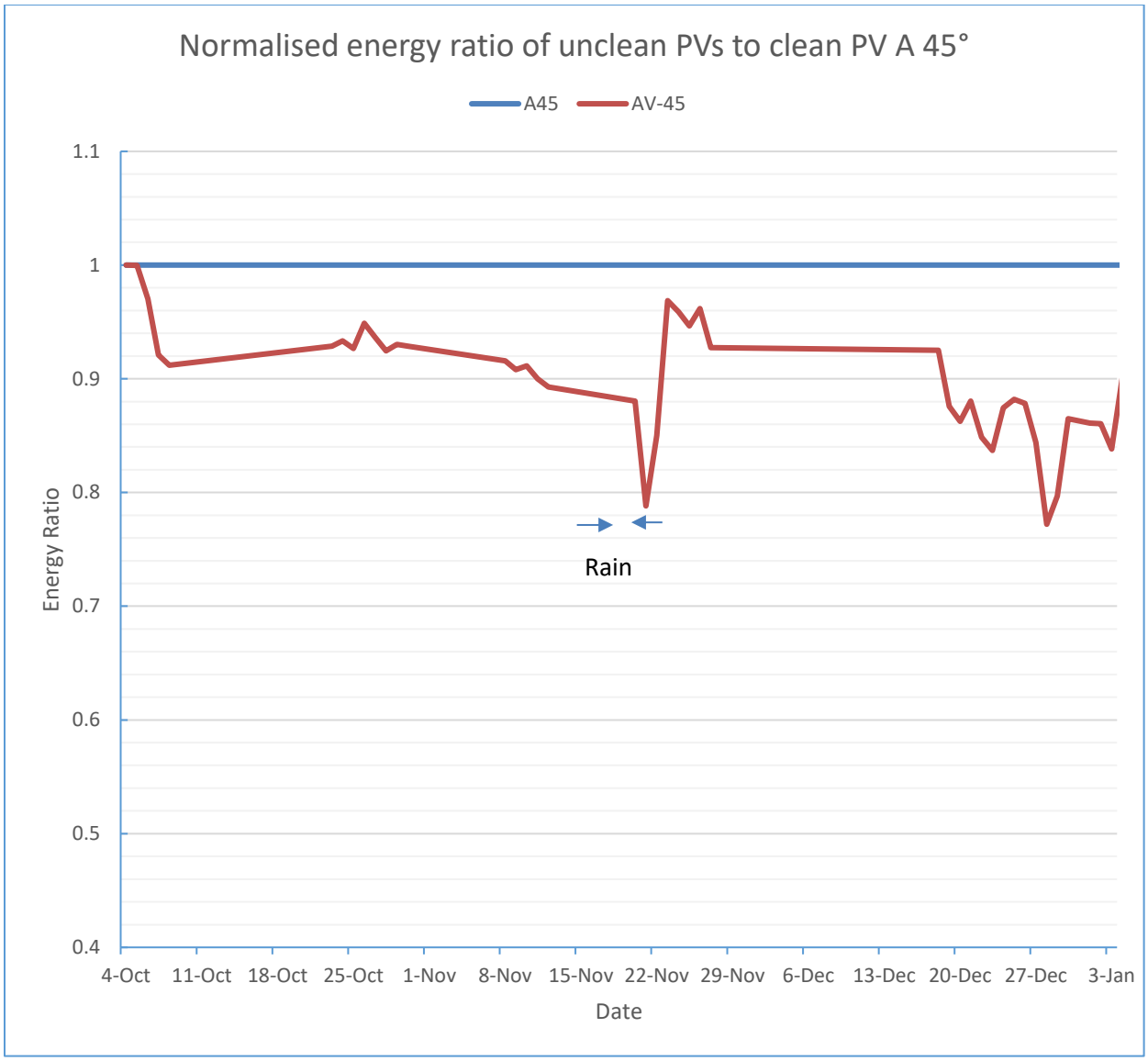

Figure 4-10 Angle 45 energy ratio of soiled PVs to clean PV A45

It is noticed from both curves the increase in the soiled PVs energy ratios after the 22nd of November, and that is because it rained on that day for two nights cleaning the PVs and restoring their output.

Even a bigger drop is noticed on the angle 30 PVs

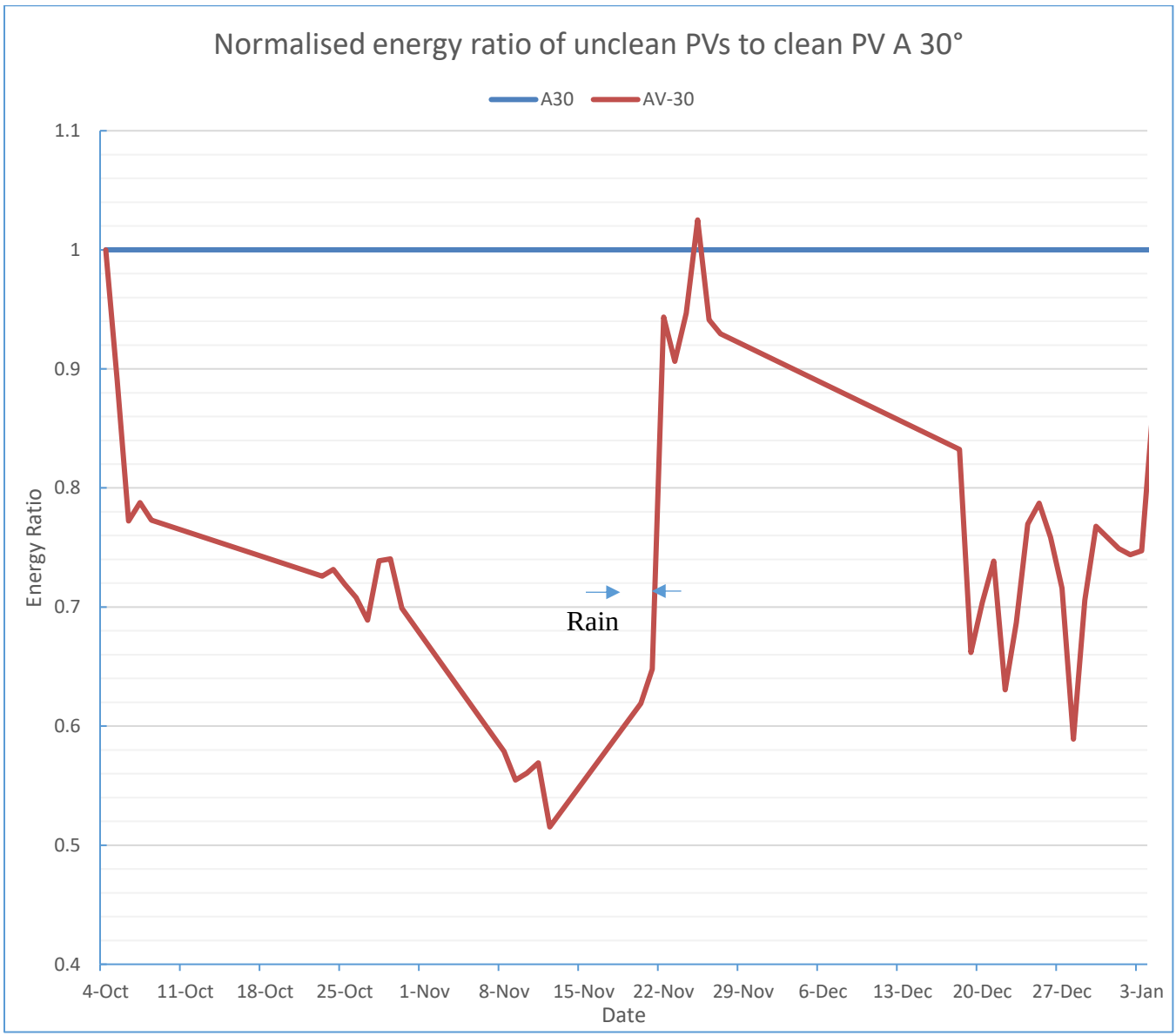

Figure 4-11 Angle 30 energy ratios of PVs soiled angle 30 PVs to clean PV A30

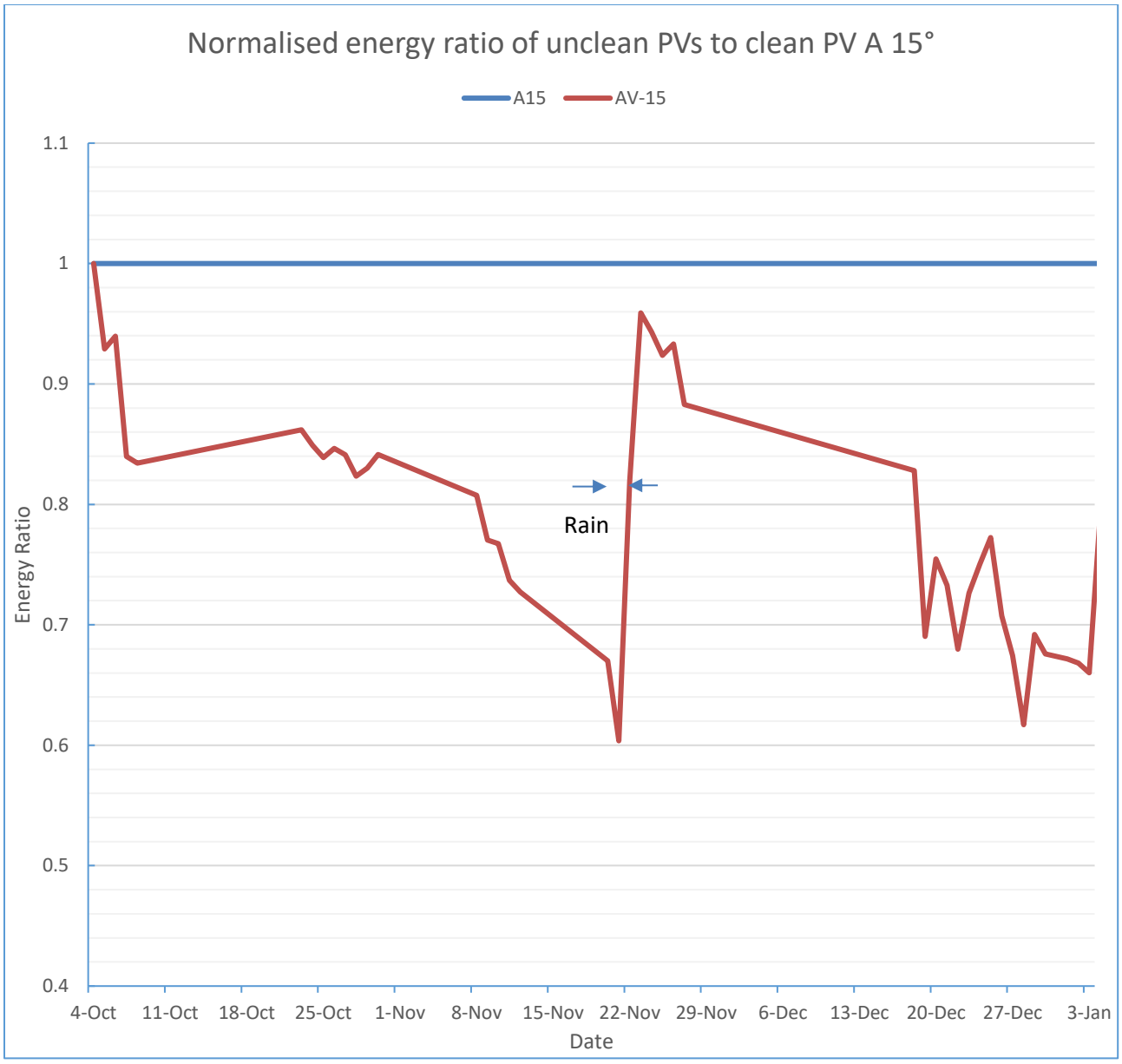

Figure 4-12 Angle 15 Energy ratio of soiled angle 15 PVs clean PV A15

The biggest drop before the rain was showed by the angle 15 and angle 30 PVs as it reached 45% decrease in energy output. This is explained by having a lower tilt angle which causes more dust to accumulate on the PV which cause a higher impact on the Performance.

Through the three months that the data logger was running, current and volt were recorded and from that the power time curve for each day was drawn. The area under each curve represented the whole energy the PV produced during the day, also the maximum power output could be identified by each PV on each single day.

The following table shows the total energy of each PV,

Table 4-1 daily total energy of each PV

	TOTAL POWER OUTPUT / WH												
Date	A	B	C	D	E	F	G	H	I	J	K	L	
4-Oct	942.9085	897.4772	897.8185	1014.968	1000.382	1000.311	900.4016	1052.721	957.2813	924.551	890.3771	770.281	
5-Oct	940.6286	896.3627	897.377	1008.009	1001.885	1001.244	800.1152	935.3191	945.6937	898.9717	810.894	790.6209	
6-Oct	1013.508	960.7047	927.5359	1081.582	1003.394	999.1638	744.0813	980.1663	1014.329	975.6862	849.8197	711.6294	
7-Oct	1043.985	980.8615	955.2462	1109.932	998.3694	991.2322	761.6498	987.2997	1017.68	967.7511	815.2328	674.4354	
8-Oct	997.0955	931.0236	898.1248	1048.266	956.519	946.8259	705.1502	924.4438	960.2018	908.7223	788.5655	648.0884	
23-Oct	987.8907	951.0854	882.2825	1043.631	976.2662	990.1687	676.5995	812.3691	981.1221	935.2765	845.7652	676.3034	
24-Oct	974.4411	917.2759	857.7442	1018.356	915.5823	922.0198	646.8829	770.8056	930.9246	849.2158	736.5726	585.5829	
25-Oct	970.3268	929.2929	866.6235	1019.741	947.8371	961.906	647.8948	785.1937	948.3015	896.7496	793.9322	624.0454	
26-Oct	992.7371	948.5261	897.3893	1035.562	968.4541	985.5639	646.9644	906.5239	962.1047	904.3235	807.8499	633.8747	
27-Oct	973.3052	914.6536	874.245	1016.909	917.6909	937.1175	615.1389	877.1648	939.853	867.1782	760.3813	585.8224	
28-Oct	1132.626	1063.222	993.7754	1145.189	1041.089	1063.076	737.7393	977.6258	1051.075	971.3373	845.3448	657.933	
29-Oct	1122.163	1051.93	992.3682	1141.106	1042.274	1062.919	731.8813	958.9477	1040.48	973.9223	858.6628	679.329	
30-Oct	1039.171	982.5765	924.2621	1070.653	971.6349	994.303	647.4448	894.8281	974.8115	912.4302	803.9306	634.0374	
8-Nov	848.7116	791.1309	756.6676	897.3978	793.6785	811.2922	451.3688		821.008	774.1493	632.5008	483.5636	
9-Nov	995.4304	931.8833	895.2429	1024.316	915.5653	940.2206	498.8539		946.4716	890.1611	732.1888	567.0351	
10-Nov	887.9505	842.4506	812.5728	955.8848	847.6139	871.4728	465.6816		874.6299	834.0583	669.4079	502.028	
11-Nov	954.7495	888.4967	850.325	990.7683	862.12	888.0687	489.9862		906.3024	844.1891	660.1175	503.9644	
12-Nov	976.4159	907.3382	864.2687	1009.614	879.9991	904.9007	450.1958		919.674	854.347	656.6165	507.9514	
20-Nov	1054.265	951.0832	900.2701	1055.116	893.3365	907.2737	349.5791	826.709	904.1131	852.4867	560.6935	438.8423	
21-Nov	362.9117	301.4324	266.7476	403.7363	282.939	295.6484	168.0693	258.0094	362.0311	279.1489	171.9925	158.8879	rained that night
22-Nov	867.7024	858.7996	858.842	918.768	873.9453	901.1627	437.6817	882.7946	850.6403	766.6999	751.6428	637.0657	
23-Nov	522.9228	520.2875	521.4763	555.0732	520.2931	538.9652	271.9189	527.1715	528.7829	453.8321	437.5231	370.7951	
24-Nov	883.1212	767.6692	812.2334	917.5075	850.9137	864.9892	335.3229	815.7879	783.2639	739.067	700.9007	550.8649	
25-Nov	689.5375	686.8449	643.1789	733.9551	683.6221	729.3866	191.8425	742.6746	658.6087	642.4397	636.4716	524.6153	
26-Nov	920.4723	911.1609	837.8586	955.9957	870.2506	882.9689	349.0044	835.7587	807.2677	702.2443	652.3897	501.5396	
27-Nov	1020.502	1009.708	927.5782	1056.681	964.4215	974.5221	333.0934	905.8029	885.9964	803.478	758.9981	592.0473	
18-Dec	944.4821	891.5093	910.3364	990.1976	900.5726	868.2538	855.6259	820.684	896.3639	815.5954	660.9938	500.1373	
19-Dec	284.5891	237.5871	236.9617	296.1114	253.7501	253.8531	251.2455	227.1589	312.034	270.3746	183.0512	186.2308	
20-Dec	457.602	403.6268	409.8049	493.2445	419.439	427.5198	412.1127	390.3066	503.9594	434.2784	312.3904	273.823	
21-Dec	677.6385	620.5546	651.6951	705.6666	618.5578	619.1412	596.5096	571.5221	703.5538	599.5322	444.5667	362.9215	
22-Dec	238.3613	193.8083	192.0726	265.3862	213.0851	218.9815	207.8606	198.6295	286.4499	249.1216	165.5834	163.8777	
23-Dec	538.2185	465.3432	479.9344	553.2137	460.3143	464.3409	432.8997	413.2329	546.9521	459.0523	320.3888	283.7925	
24-Dec	466.2312	422.8189	452.1831	492.7217	439.4747	422.218	430.5006	413.8701	488.8328	455.4648	359.9212	311.0959	
25-Dec	1071.299	977.6815	980.1932	1079.031	959.7429	926.1196	886.1823	850.2201	981.8267	866.8166	659.7823	520.5489	
26-Dec	1237.692	1134.734	1194.444	1230.313	1083.452	1050.431	997.8886	954.9596	1144.587	956.9386	693.9746	572.601	
27-Dec	645.5008	564.0422	512.118	654.83	535.0274	513.282	471.2555	431.5425	547.923	481.7398	319.0948	263.9058	
28-Dec	204.059	158.9017	141.2626	230.0968	171.3876	170.258	164.7237	153.3688	236.6972	210.8959	127.6418	126.8955	
29-Dec	758.9633	672.9093	699.6212	780.3013	654.0044	646.27	618.9152	597.8413	770.1127	661.4116	458.5229	388.2765	
30-Dec	821.8478	731.0878	752.2327	824.2932	728.7747	678.4432	672.8521	625.658	740.6606	656.764	445.1398	381.1909	
31-Dec	1099.765	992.9369	1010.476	1112.995	961.8143	930.15	882.6797	842.275	1013.863	877.6878	608.4168	516.48	
1-Jan	854.3888	766.9744	760.1295	885.3649	769.5767	746.5895	719.7071	676.6739	821.0966	711.9274	475.585	425.9882	
2-Jan	785.0054	685.5505	683.4296	777.8126	669.329	630.6364	607.5572	567.792	693.8208	601.1786	390.7298	351.4498	
3-Jan	1074.228	961.4137	994.6664	1092.973	928.1689	901.5701	874.6145	820.033	997.593	866.8826	562.905	495.9809	rained that night
4-Jan	816.9218	786.7422	883.3353	868.1942	834.7183	799.9391	823.7052	798.1379	835.3429	754.8683	694.3867	602.7871	

From this table the energy ratio was calculated as a ratio of the clean PV to compare how the performance was varied only due to the dust accumulation. As shown in the following table;

Table 4.2 normalized energy ratios

	normalized energy ratio (correction factor)										
A	B	C	D	E	F	G	H	I	J	K	L
1	1	1	1	1	1	1	1	1	1	1	1
1	1.003095	1.00423	1	1.003965	0.995514	0.890591	0.899118	1	1	0.911135	0.946751
1	0.99779	0.963341	1	0.937081	1.003322	0.772179	0.878472	1	1	0.879795	0.999401
1	0.988985	0.963158	1	0.908573	0.93313	0.787808	0.881952	1	1	0.850908	0.828822
1	0.98288	0.948148	1	0.921694	0.902078	0.773029	0.875236	1	1	0.876539	0.791943
1	1.013414	0.940102	1	0.944901	0.912354	0.725914	0.752727	1	1	0.913429	0.810439
1	0.990879	0.926571	1	0.908161	0.958357	0.731455	0.752727	1	1	0.876117	0.821711
1	1.008117	0.940132	1	0.938877	0.914546	0.719175	0.752727	1	1	0.894287	0.783588
1	1.005753	0.951531	1	0.944643	0.952813	0.707839	0.856573	1	1	0.902343	0.790792
1	0.9892	0.945498	1	0.911547	0.961332	0.688953	0.848455	1	1	0.885703	0.79652
1	0.988129	0.923588	1	0.918281	0.930844	0.738832	0.845563	1	1	0.87908	0.767671
1	0.98675	0.930879	1	0.922616	0.937674	0.740429	0.837854	1	1	0.89056	0.769713
1	0.995304	0.936234	1	0.916683	0.94089	0.699131	0.8345	1	1	0.889987	0.792635
1	0.981216	0.938472	1	0.893356	0.938069	0.578709		1	1	0.82528	0.789646
1	0.985433	0.946687	1	0.902859	0.913182	0.554807		1	1	0.830844	0.709817
1	0.998693	0.963274	1	0.895689	0.927172	0.560456		1	1	0.810698	0.723867
1	0.979587	0.937501	1	0.878942	0.920901	0.569098		1	1	0.789853	0.683989
1	0.978162	0.931731	1	0.880423	0.905397	0.515281		1	1	0.776323	0.678387
1	0.94961	0.898876	1	0.855224	0.905337	0.407004	0.831261	1	1	0.664359	0.675624
1	0.87431	0.773706	1	0.70788	0.868566	0.488674	0.647884	1	1	0.622355	0.584976
1	1.041831	1.041883	1	0.960823	0.739678	0.541613	0.943455	1	1	0.990264	0.646803
1	1.047327	1.04972	1	0.94681	0.990746	0.5413	0.90632	1	1	0.973802	0.944226
1	0.915019	0.968137	1	0.936787	0.980788	0.450642	0.94684	1	1	0.957938	0.928445
1	1.048521	0.981862	1	0.940831	0.952283	0.306615	1.025129	1	1	1.000717	0.846991
1	1.041983	0.958156	1	0.919503	1.003814	0.455082	0.941176	1	1	0.938391	0.927953
1	1.041497	0.956782	1	0.921908	0.932941	0.39574	0.929414	1	1	0.954183	0.811586
1	0.993593	1.014576	1	0.918675	0.931563	1.004792	0.832337	1	1	0.81863	0.837336
1	0.878782	0.876468	1	0.865597	0.885706	0.847565	0.661813	1	1	0.683867	0.696838
1	0.928471	0.942683	1	0.858957	0.865948	0.860789	0.704073	1	1	0.726598	0.782714
1	0.963958	1.012332	1	0.885412	0.875505	0.892476	0.738487	1	1	0.749013	0.716505
1	0.85588	0.848215	1	0.811035	0.886247	0.763836	0.63038	1	1	0.671383	0.687888
1	0.910104	0.938641	1	0.840478	0.833477	0.833133	0.686836	1	1	0.704985	0.747525
1	0.954618	1.020915	1	0.900942	0.84783	0.927022	0.769681	1	1	0.79821	0.702516
1	0.960645	0.963113	1	0.898433	0.865565	0.95009	0.787234	1	1	0.768844	0.77617
1	0.965068	1.01585	1	0.889526	0.866958	0.917719	0.758479	1	1	0.732528	0.68242
1	0.919795	0.835122	1	0.825301	0.862416	0.905343	0.715997	1	1	0.669071	0.679963
1	0.819689	0.728699	1	0.752374	0.791758	0.732554	0.589049	1	1	0.61135	0.622521
1	0.933281	0.970328	1	0.84661	0.747415	0.845967	0.705731	1	1	0.700251	0.683747
1	0.936385	0.963468	1	0.893051	0.836597	0.956262	0.767936	1	1	0.684624	0.667093
1	0.950382	0.967169	1	0.872896	0.831374	0.916432	0.755235	1	1	0.700206	0.659554
1	0.944934	0.936501	1	0.878	0.844159	0.922652	0.749191	1	1	0.674772	0.668699
1	0.91927	0.916426	1	0.86922	0.851774	0.921757	0.743959	1	1	0.656505	0.679953
1	0.942085	0.974669	1	0.857793	0.818972	0.922868	0.747283	1	1	0.655903	0.66432
1	1.013744	1.138208	1	0.971153	0.833211	1.037967	0.868601	1	1	0.92917	0.650163

The energy ratio is used with a correction factor so that all PVs start from one and see how that 1 is effected as time goes by, it rained twice during the experiment and that rain caused a high surge in the energy ratio of all PVs , emphasizing on the effect of dust accumulation on energy output.

The maximum power output was not affected by a great deal by the dust accumulation as the total energy output. The following graphs will show this, the first curve is the power time curve and the major differences of the power would be in the beginning and the end of the day.

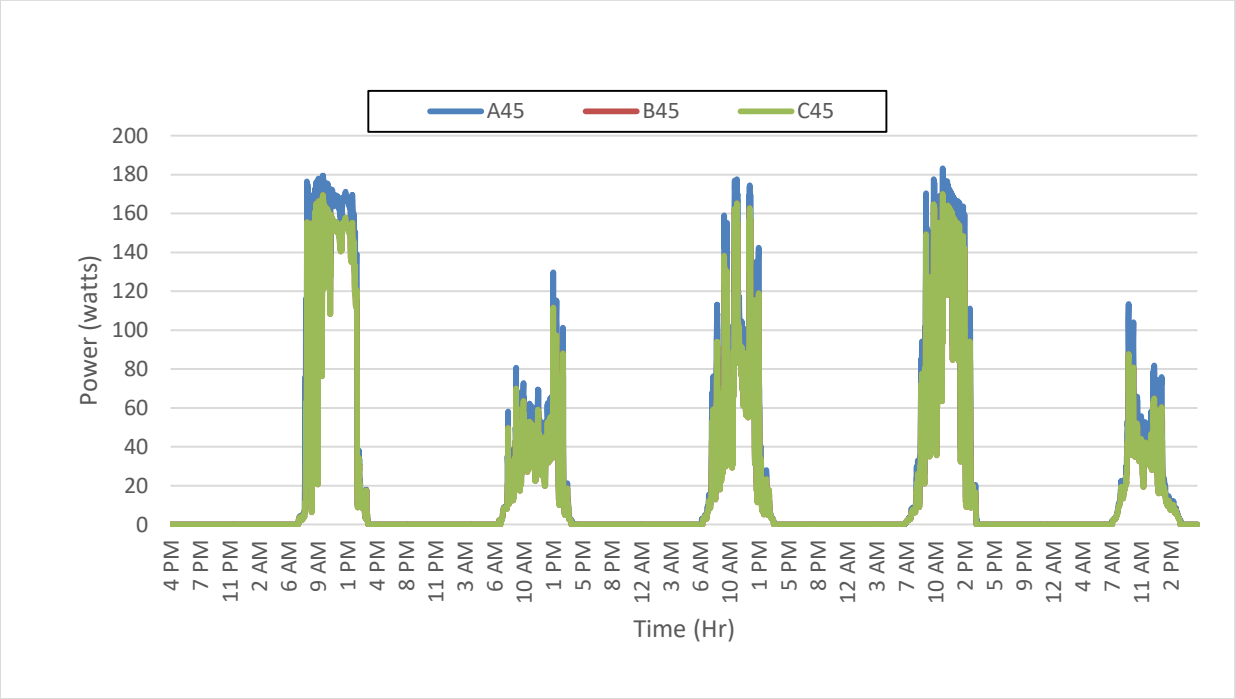

Figure 4-13 power time curves for PVs at angle 45 degrees from 18th to 22nd of December

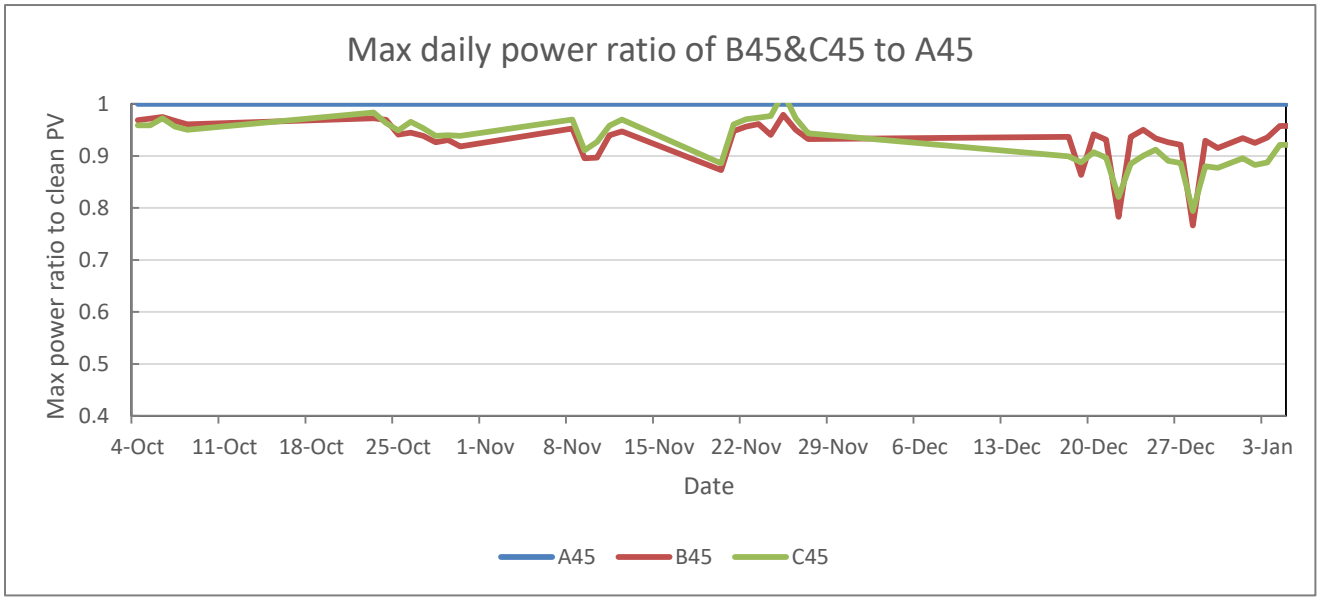

Figure 4-14 angle 45 PVs maximum power output of ratios of E&F to clean PV D

The maximum power ratios were as seen in fig (4.14) the maximum drop in power output ratio was by B45 which dropped to 80%, but in the energy drop the maximum drop was by B45 as well which dropped to 70% and 74% on the day on which it showed an 80% drop on maximum power output.

As the angle gets lower more dust accumulate on the PV panel and thus higher drop in the ratio will be noticed, the following show the energy and maximum power output ratios of the angle 15 PVs;

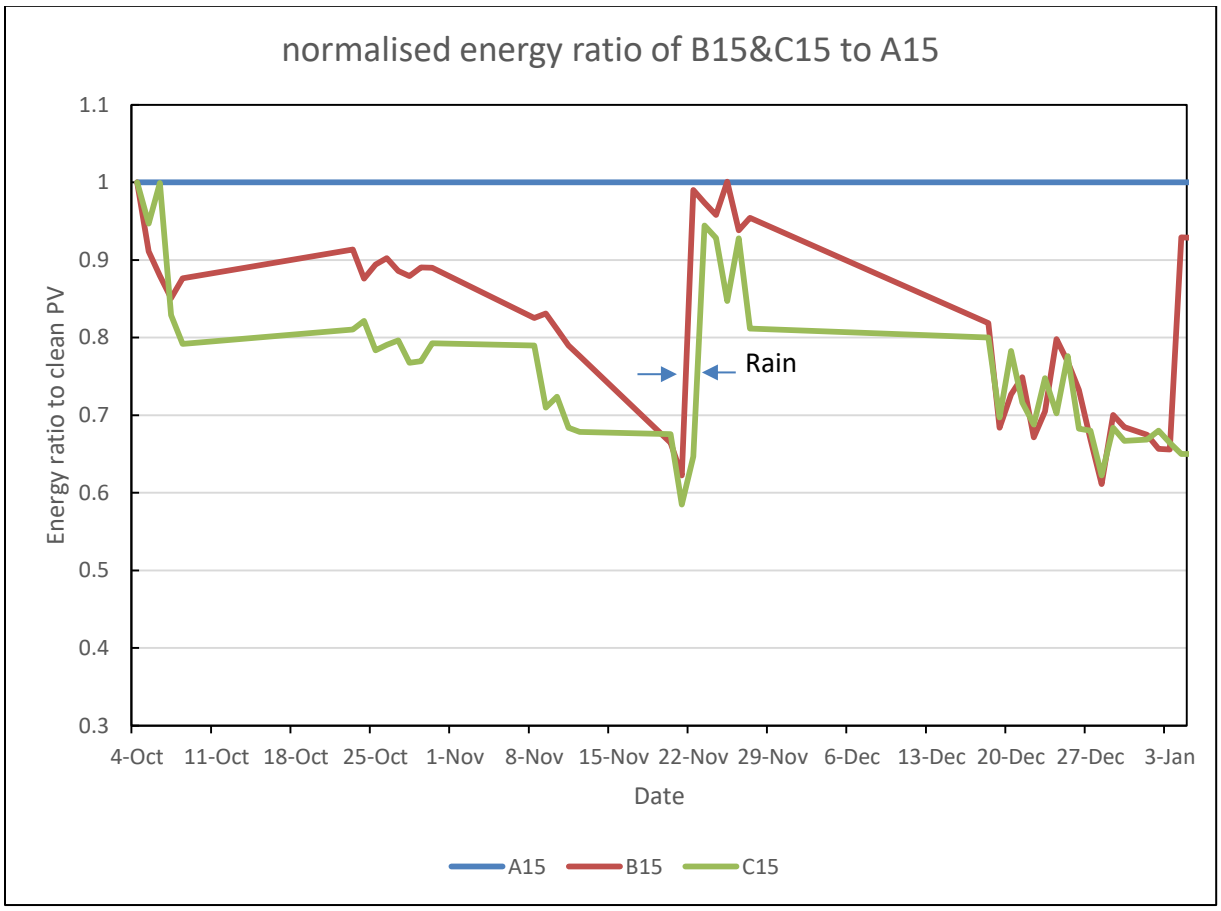

Figure 4-15 energy ratios of angle 15 PVs where B15andc15 are ratios to clean PV A15

As seen from figure (4-15) and fig. (4-16) the maximum power output is not effected by performance deterioration strongly, or by dust accumulation, in the same manner as the total energy. The reason for this is that the maximum power occur at solar noon when the sun is vertical on the PVs, and hence the ray scattering effect that is done by the dust particles is minimal. This indicates that the angle of incidence of the solar radiation has an effect on the deterioration of the performance of the soiled PV.

Also it is noticed that the drop in the angle 15 reached as low as 60% which is 10% lower than the biggest drop by the angle 45, which shows that the dust accumulation has a higher effect on lower angles

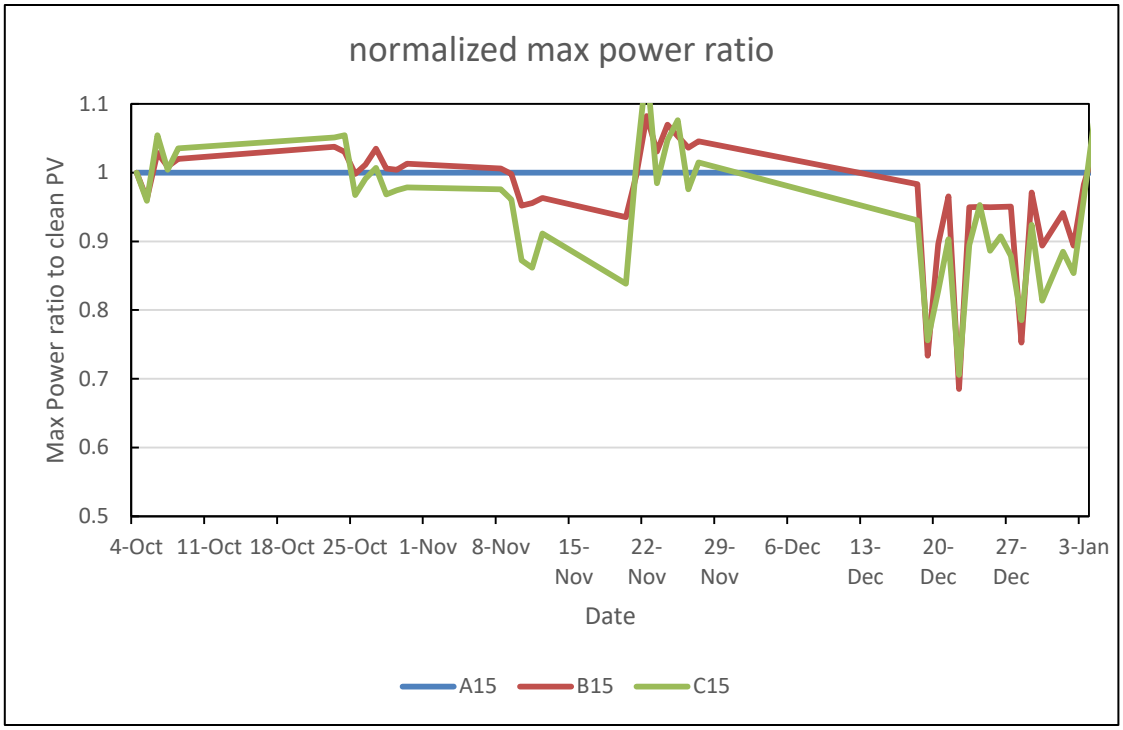

Figure 4-16 normalized maximum power output of angle 15 PVs A15 clean, B15andC15 not cleaned

All PVs experienced a rise in their performance ratios (energy as a ratio to their clean counterpart) after the rain, it rained twice during the run, 22nd of November until the 23rd, and on the 4th of January. This backs the explanation of the deterioration of performance due to dust accumulation on the PVs.

Chapter 5

5. Analysis of measured data

5.1 effect of dust accumulation on Power, Daily energy, and hourly performance

5.1.1 Energy analysis

To further study the effect of the dust accumulation, the normalized energy ratios of the clean PV to the average of the two soiled PVs is plotted over the course of the experiment for all angles.

The energy ratios are normalized with a correction factor so they all start at 1 and then the difference in energy output at each angle is varied with the other variables. As shown in the previous chapter.

Diffuse radiation effect

Another point to be considered with total daily energy, is that the ratio is fluctuating between the clean and unclean PVs in some consecutive days. When the weather conditions were examined on those days from the weather station it was found that on clear days the energy ratio of the unclean PVs is higher than those on cloudy days. The weather station would show how a day is clear or cloudy from the solar radiation readings. The explanation to this phenomena would be that on clear days the sun radiation that is hitting the PVs is mostly beam radiation so it can penetrate the dust layer and improve performance, while on cloudy days the solar radiation is mostly diffuse which is mostly reflected by the glass and causes the deterioration.

This was concluded from studying two consecutive days one with clear skies followed by one with cloudy skies and examine how the performance of the PVs varied over the two days. This was repeated with another set of days to verify the results. This was done with the hourly power ratios, to see how each PV is performing throughout the day.

Two consecutive days were examined to make sure that any change in performance was due to the clearness index and not due to change in the thickness of the dust layer on the PV.

The first two days that were examined were the 20th and 21st of November. To determine first that the t 20th sky was clear and 21st was not, the solar radiation over the whole day is plotted as shown in Fig.(5-1);

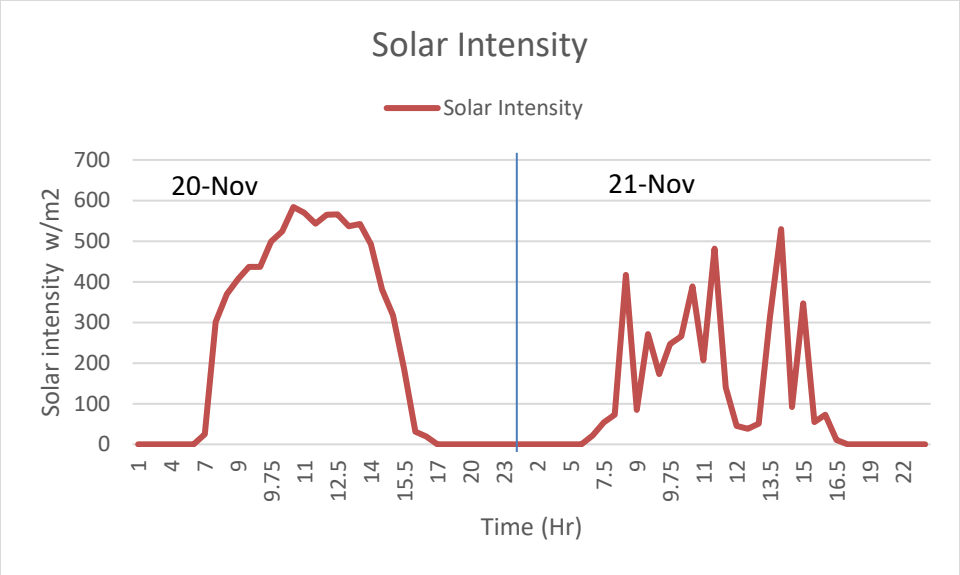

Figure 5-1 solar intensity vs. time of day for 20and21 of November

This graph shows that on the 20th the solar intensity was constant and not fluctuating as on the day after, and this fluctuation in solar intensity shows cloudy skies. Next step was to calculate the clearness index which from the ratio of diffuse rays could be identified.

The following equation was used to calculate the clearness index; [11]

$$K = G / G_o \qquad \text{(Eq. 5.1)}$$

Which is the solar radiation on the ground over the extraterrestrial radiation. The radiation on the ground is already recorded by the weather station, the extraterrestrial radiation could be calculated from the following equation; [11]

$$G_o = G_{sc}\left(1 + 0.033\cos\frac{360n}{365}\right)\cos\theta_z \qquad \text{(Eq. 5.2)}$$

Where,

Θz, is the **Zenith angle**, the angle between the vertical and the line to the sun, that is, the angle of incidence of beam radiation on a horizontal surface.

G_{sc}, the solar constant which is 1353 W/m2 with an estimated error of ±1.5%.

n , is the day number , with jan 1st is 1 and December 31st is 365

To calculate *Θz the* following equation (eq.5.3) was used;[11]

$$\cos\theta_z = \cos\phi\cos\delta\cos\omega + \sin\phi\sin\delta \qquad \text{(Eq.5.3)}$$

Where,

φ **Latitude**, the angular location north or south of the equator, north positive; $-90^\circ \le \varphi \le 90^\circ$.

δ **Declination**, the angular position of the sun at solar noon (i.e., when the sun is on the local meridian) with respect to the plane of the equator, north positive; $-23.45^\circ \le \delta \le 23.45$.

ω **Hour angle**, the angular displacement of the sun east or west of the local meridian due to rotation of the earth on its axis at 15° per hour; morning negative, afternoon positive.

After calculating the clearness index the ratio of diffuse beam was extracted from the following curve;

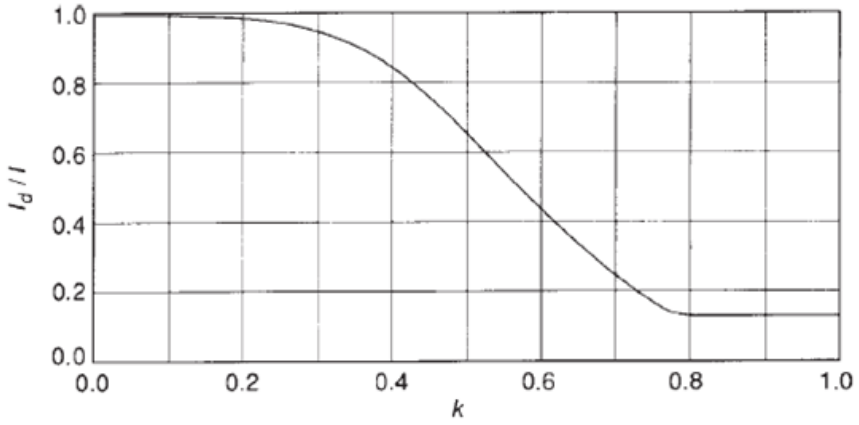

Figure 5-2 the ratio Id/I as a function of hourly clearness index k. From Erbs et al. (1982).[11]

After the diffuse ratio was extracted from the graph, the hourly diffuse ratio was plotted against the hourly power ratio of the PVs for the two days under consideration.

For each angle the hourly energy ratio (the soiled PVs energy ratio to the clean PV) was plotted along with the hourly diffuse radiation ratio.

The following are these curves;

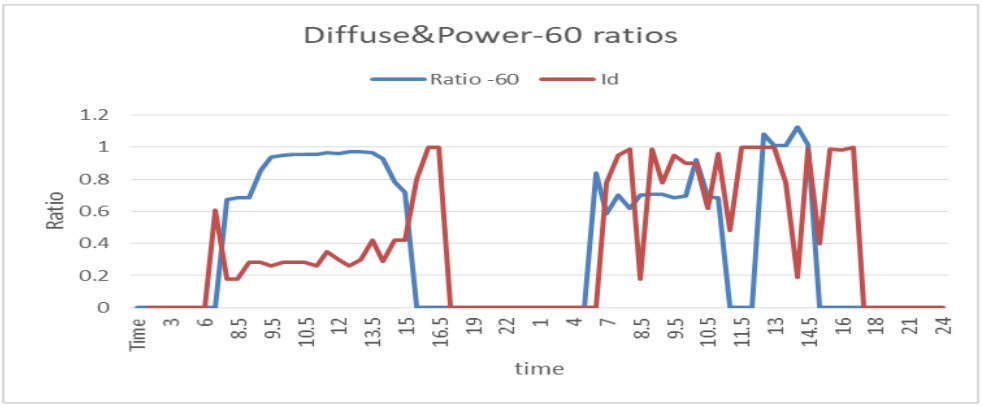

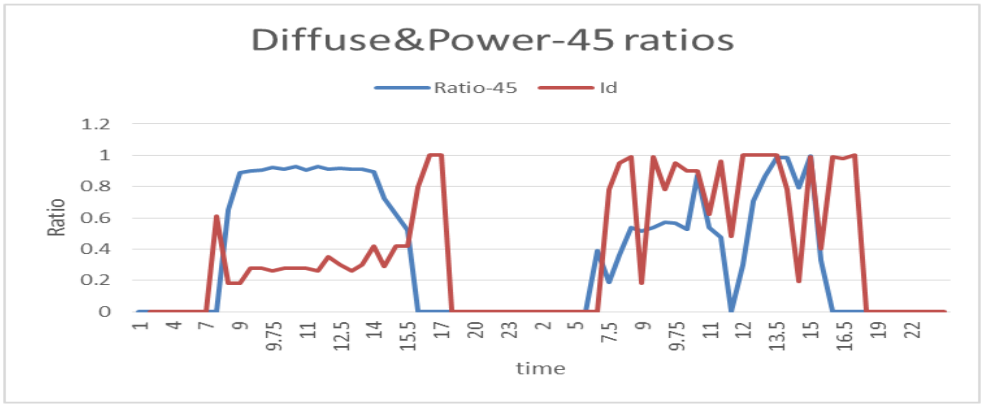

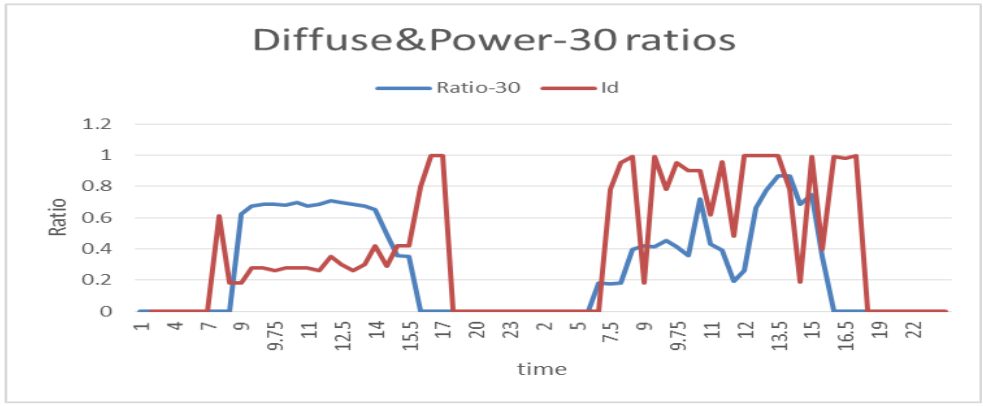

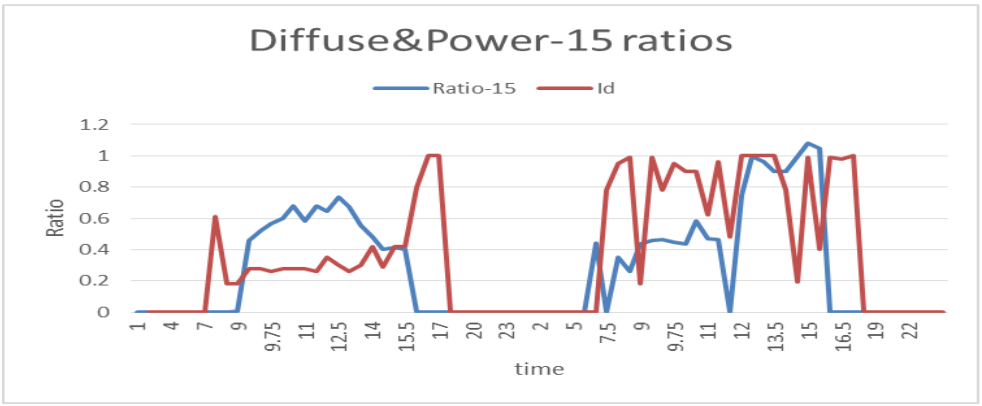

Figure 5-3 hourly power and hourly diffuse radiation ratios for different angle PVs

It is noted from the previous curves, Fig. (5-3), that when the diffuse radiation ratio was low, i.e. high clearness index, on the first day the energy ratios were all higher than on the second day when the diffuse ratio got up. Even though these are two consecutive days, there is a noticeable drop in energy ratios and that is explained by the diffuse beam radiation ratios changes due to the change in the clarity of the sky. Another set of days were examined to verify this analysis. The two days were 18th and 19th of December.

The same procedure was followed the clearness index was calculated from the ratio of the solar radiation recorded by the weather station to the extraterrestrial radiation, and from that the hourly diffuse ratio is deduced. The solar radiation of these days was as follows;

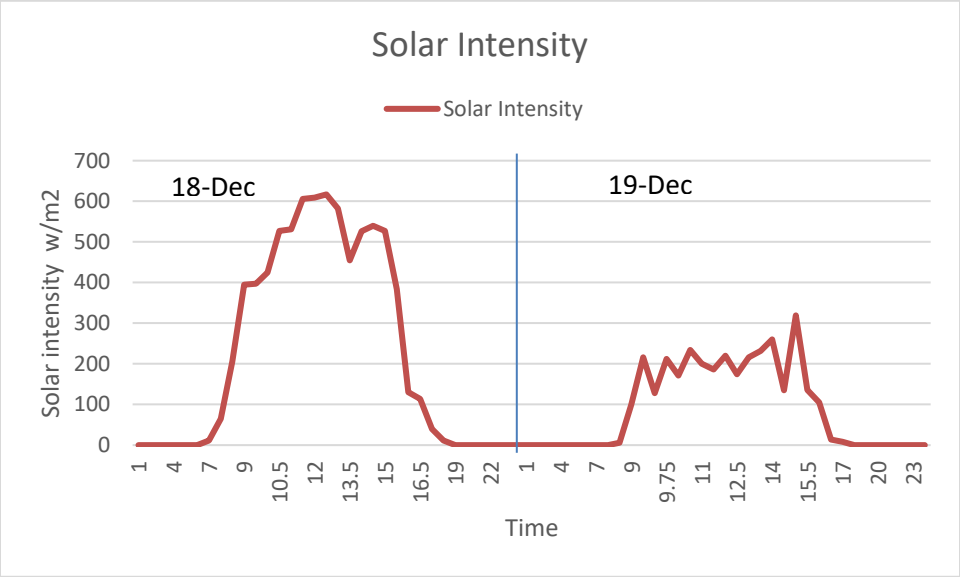

Figure 5-4 hourly solar intensity of 18and19 December

The two days will give the required as the solar intensity shows a clear sky on the 18th and a cloudy weather on the 19th of December. The hourly diffuse ratio was calculated as the precious set of days, The curves are as follows; as shown in Fig (5-5);

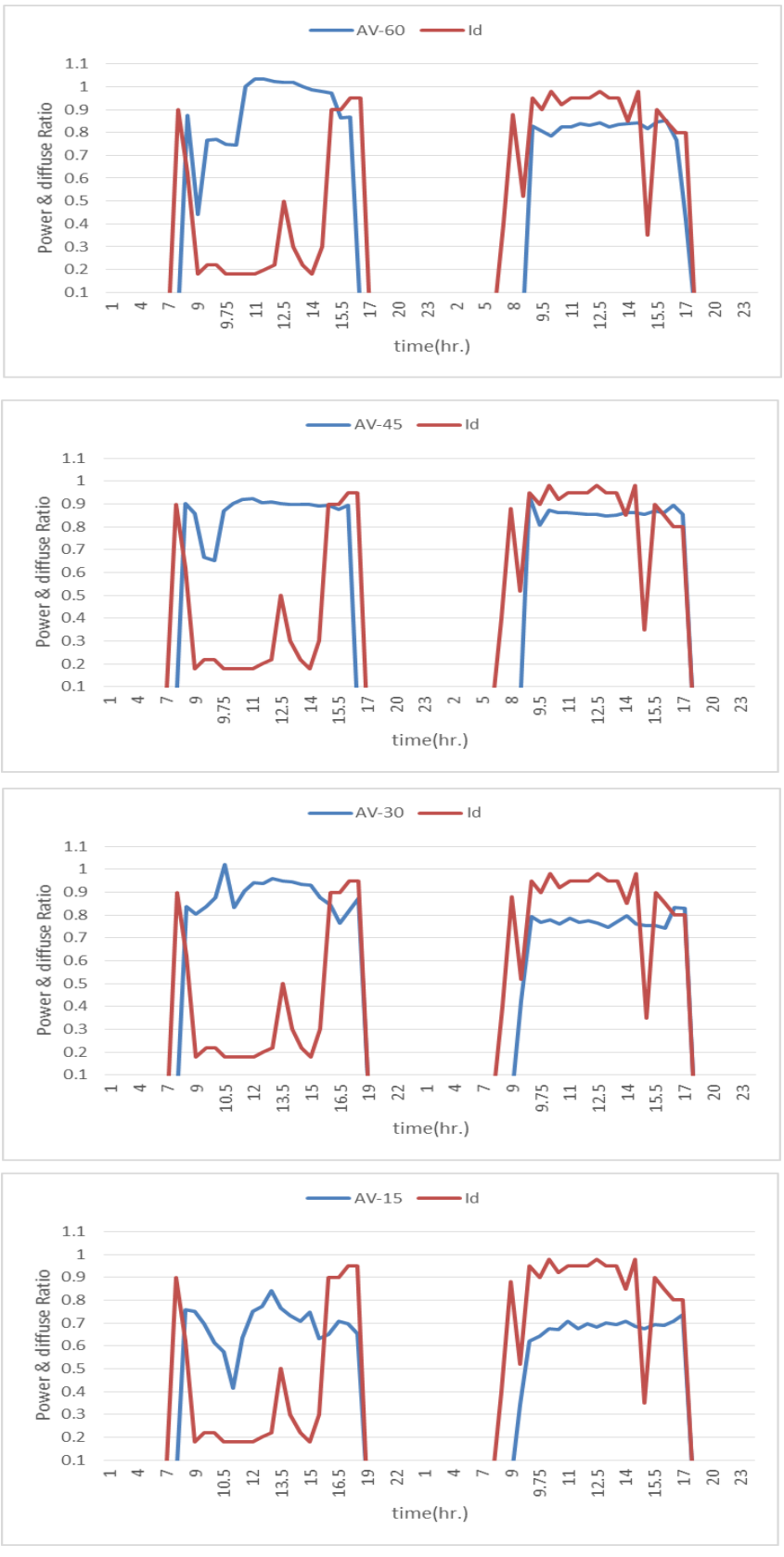

Figure 5-5 hourly power ratio (soiled average to clean PV) against diffuse radiation ratio for all 4 tilt angles

The graphs in Fig (5-5) show the same pattern as the first set of days, on the second day where the I_d ratio was high the power ratio dropped. This was noticed for all angles, but the difference was in the percentage in the drop, for example the 60 degrees PVs dropped with an average 10% compared to a 20% drop in the 30 degrees PVs. Never the less all power ratios dropped on the cloudy day, and that verifies the effect the diffuse beam has on unclean PVs.

5.1.2 Power analysis

Angle of incidence effect

The power ratio between the unclean PVs and the clean PV is not constant through the day, when analyzed it starts low and picks up and during peak solar hours, the power output is almost the same. After that the power of the unclean starts to drop below the clean PVs. This can be explained by the fact that at solar noon or solar peak hours the solar radiation angle of incidence is at its lowest so the reflection effect the dust layer is minimal and all the radiation is utilized by the PVs, making the power output of the clean and unclean very close.

First to calculate the angle of incidence, Eq.5.4 is used [14]

$$\begin{aligned}\cos\theta = {} & \sin\delta\sin\phi\cos\beta - \sin\delta\cos\phi\sin\beta\cos\gamma \\ & + \cos\delta\cos\phi\cos\beta\cos\omega + \cos\delta\sin\phi\sin\beta\cos\gamma\cos\omega \\ & + \cos\delta\sin\beta\sin\gamma\sin\omega\end{aligned} \qquad \text{(Eq.5.4)}$$

Where,

γ ,**Surface azimuth angle**, the deviation of the projection on a horizontal plane of the normal to the surface from the local meridian, with zero due south, east negative, and west positive; $-180^\circ \le \gamma \le 180^\circ$.
ω, **Hour angle**, the angular displacement of the sun east or west of the local meridian due to rotation of the earth on its axis at 15◦ per hour; morning negative, afternoon positive.
Θ, **Angle of incidence**, the angle between the beam radiation on a surface and the normal to that surface.
φ **Latitude**, the angular location north or south of the equator, north positive; $-90^\circ \le \varphi \le 90^\circ$.
δ **Declination**, the angular position of the sun at solar noon (i.e., when the sun is on the local meridian) with respect to the plane of the equator, north positive; $-23.45^\circ \le \delta \le 23.45^\circ$.
β **Slope**, the angle between the plane of the surface in question and the horizontal; $0^\circ \le \beta \le 180^\circ$. ($\beta > 90^\circ$ means that the surface has a downward-facing component.)

The graphs shown in Fig. (5-10) show the power output ratio per hour of the day against the angle of incidence;

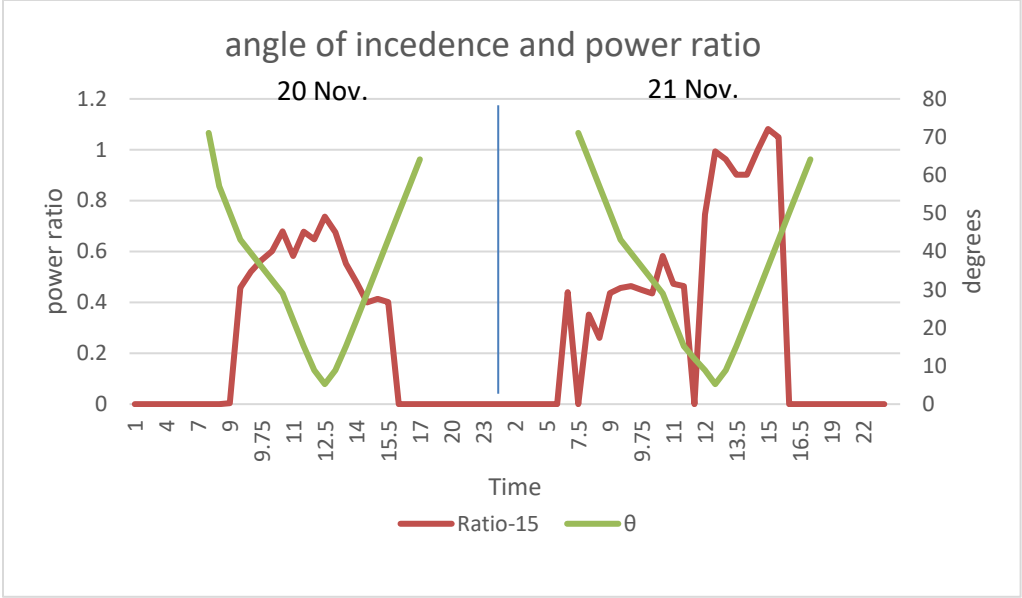

Figure 5-6 soiled to clean PV power ratio against incidence angle ϑ

As seen in Fig (5-6) the power ratio increased at noon until it reached almost one in the angle 15 and 1 in the angle 45, this is due the fact the angle of incidence is lowest at solar noon. This shows the inverse relationship between the power ratio and θ. Fig (5-7) shows the solar radiation while Fig (5-8) shows the power drop ratio ($\frac{Pclean-Psoiled}{Pclean}$) against θ during one day, the 18th of December.

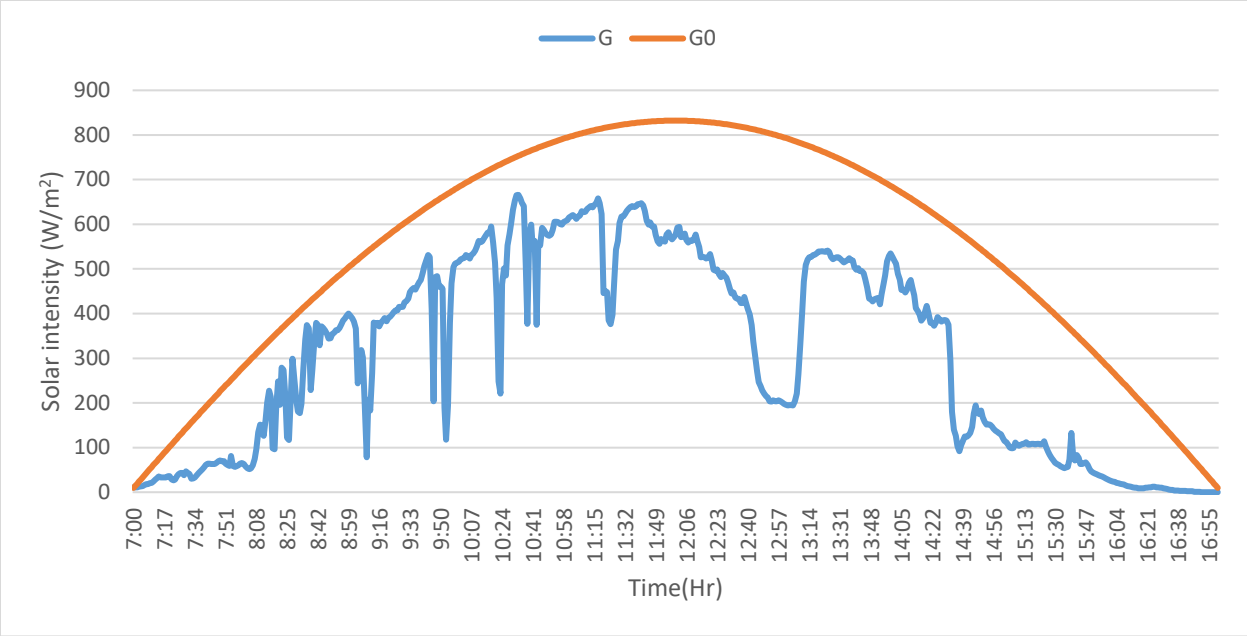

Figure 5-7 Extraterrestrial solar radiation against solar radiation measured by the weather station

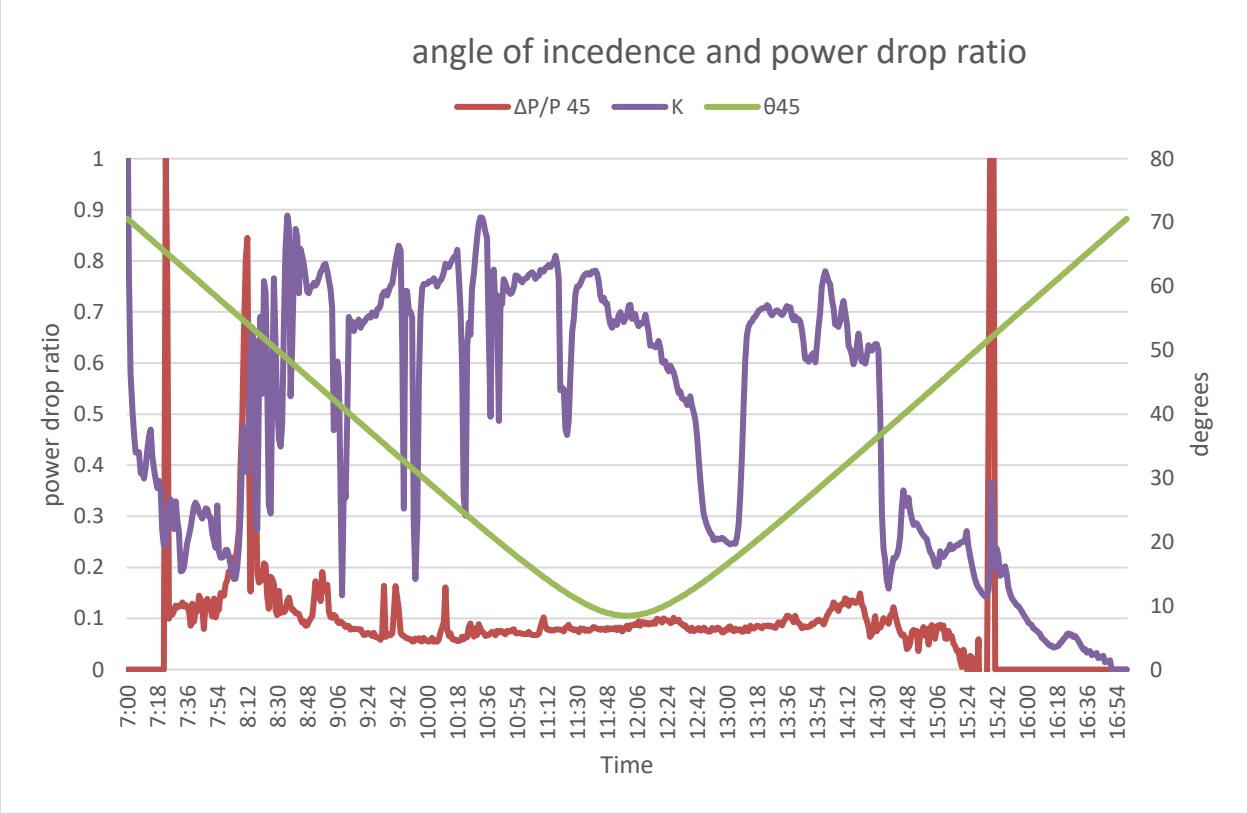

Figure 5-8 power drop ratio ($\frac{Pclean-Psoiled}{Pclean}$) against ϑ

As seen in fig(5-7) and fig (5-8) the drop between the clean and the soiled starts high in the early hours of the day , and then decrease, until noon and then starts to increase again , and then after 3 PM the solar radiation becomes very low to be picked up by the PVs so the ratio drops to zero.

To further show this effect the power outputs of all tilt angles for the 20th of November were plotted against the angle of incidence and of time of day, as shown in fig (5-9).

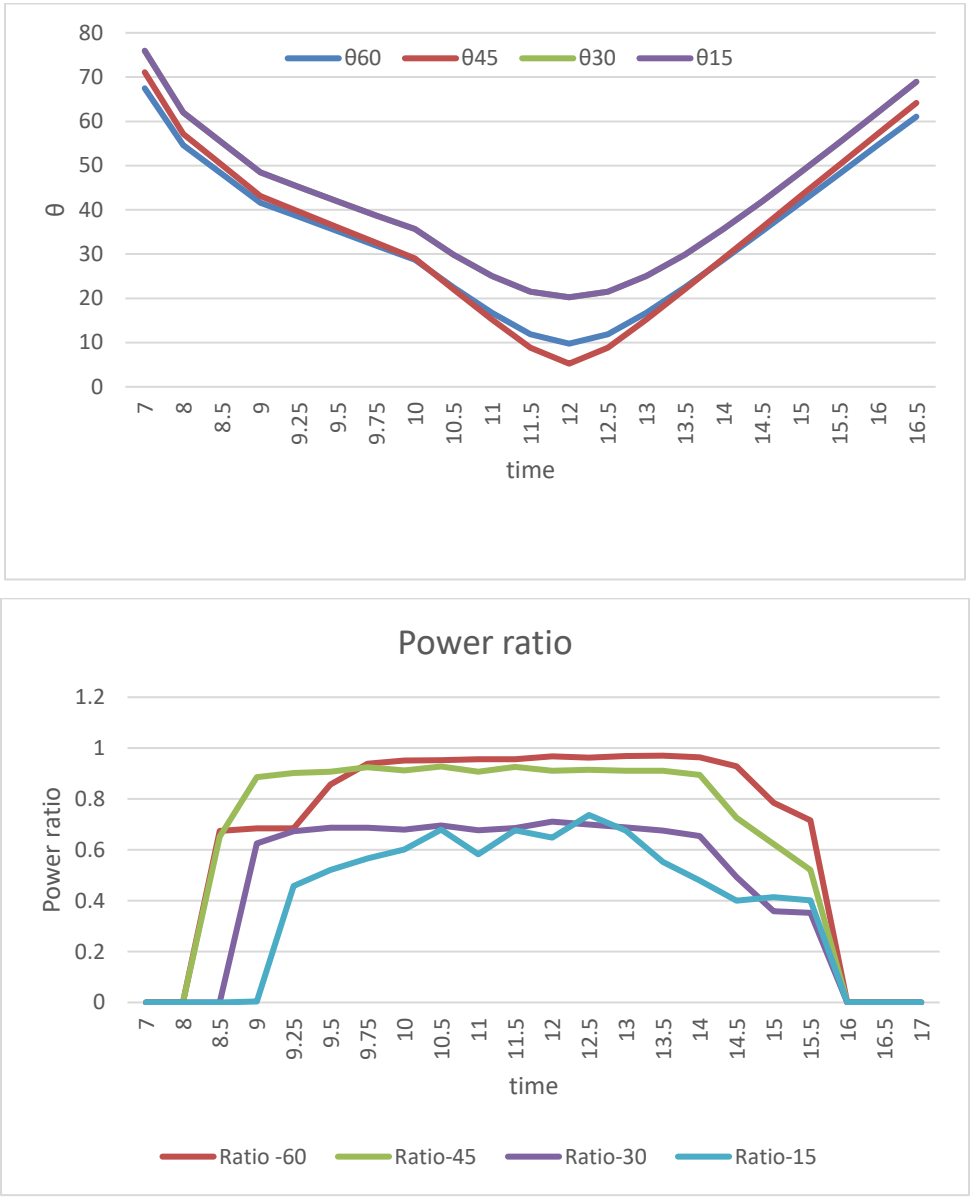

Figure 5-9 all four angles unclean to clean power ratios against angle of incidence for the 20th of November

To further illustrate how the performance of the soiled PVs change during the day Figure (5-10) shows the power ratios of the angle 60 PVs against time, from the period of the 18th till the 22nd of December. It is noted what was explained earlier in the chapter, that the ratio approaches one, ie the soiled PV is producing the same power as the clean PV at noon. That behavior is explained by the fact that the lowest angle of incidence of solar radiation is at noon. This decrease the fraction of the solar beam reflected and thereby, most of the sun rays penetrate the glass and is utilized.

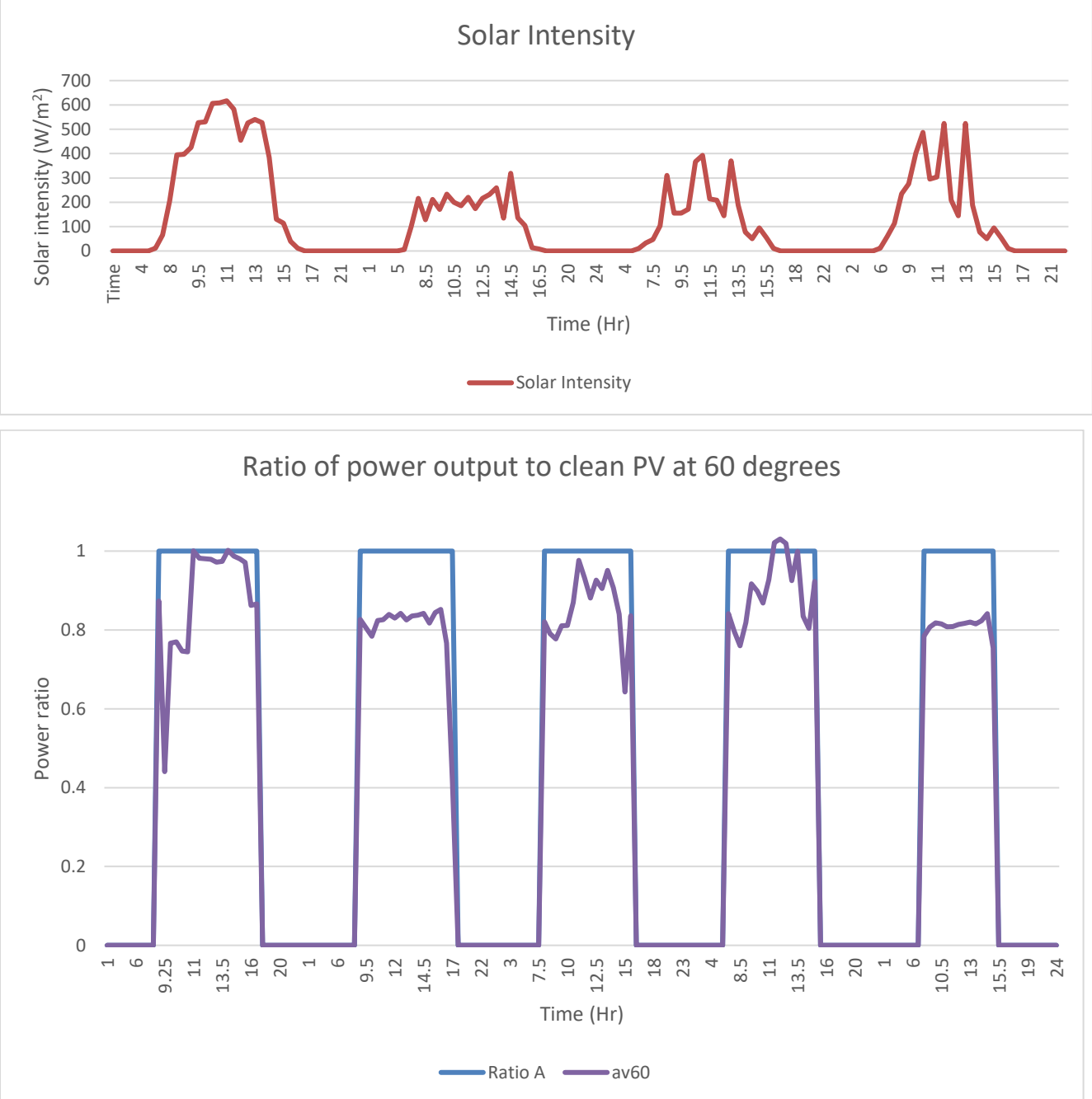

Figure 5-10 power ratio of unclean PVs AV60 clean PV A60 at angle 60 showing spikes at noon when clear sky and low angle of incidence and then dropping back during the rest of the day, power ratios from 18-22 of December

5.2 impact of performance on utilizability

It was concluded that different angles experienced different drops in power and energy outputs, but that could have a much greater impact if utiliziabitlty concept is taken into account. Utiliziabilty is the threshold solar radiation required to operate or produce useful energy, the soiling effect the amont of utilized radiation and thus the power output. An example would be the 19th of December even though the power drop was by 20% on average for the angle 60 non clean PVs, if a power threshold was taken for example to be 35 Watts, the utilizabilty of the dirty PVs for a single hour would be as follows;

The hour to be considered for example would be from 11 am to 12 pm

Utilizability = $\frac{(power-35)}{Power}$

The utilizabilty of this hour for PV A (clean) was 22%, and dropped for B (unclean) to 11.8% this represent a 50% drop in utilizabilty.

For the same hour for the PVs at angle 15 the utlizabilty was also calculated.

The utilizabilty for the same hour for A15 was 22% and dropped with unclean PVs to 2%, this huge impact on utlizabilty is due to the soiling effect.

5.3 regression model analysis

As discussed previously in this chapter the soiled PV's output relative to the clean PV on the same conditions is influenced by three factors, which are; the tilt angle (β), the clearness index of the day examined (K) and the time (t) it has been left without cleaning or rain.

Thereby, the change in daily energy output of a PV (Eclean – Esoiled) is a function in β, K and t.

In this model some assumptions are made, first of all that the relation between time and the ΔE will reach saturation after a specific period of time, meaning that after a specific period there will be no more drop in energy produced by the soiled PV relative to the clean PV. This would be due to the fact that the PV panel has accumulated the maximum thickness of dust layer possible, and after that the wind would remove any excess particles. There by, in this correlation the thickness of the dust would be represented by the time left without cleaning or rain. The relation between time and ΔE is assumed to be a growth saturation model, and should look like shown in fig (5-11)

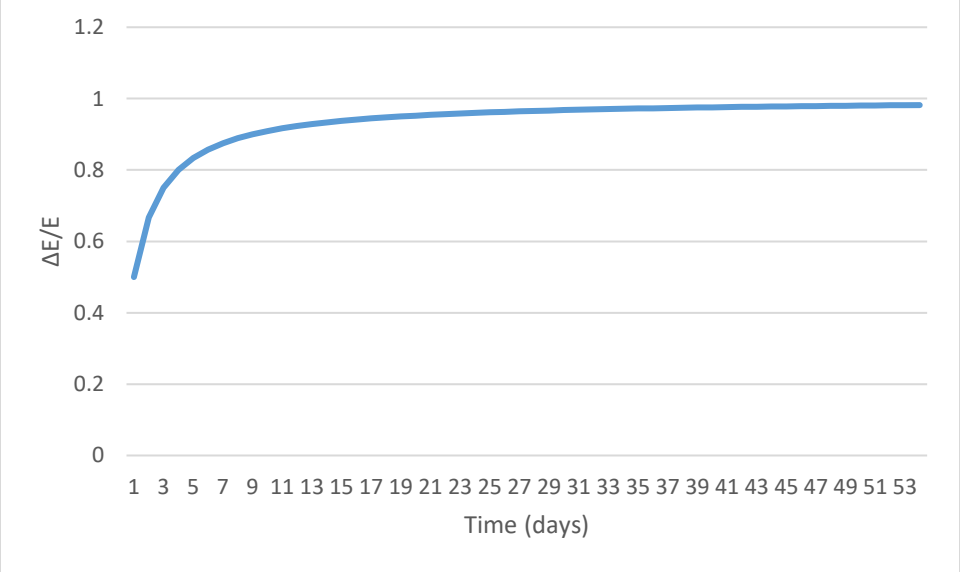

Figure 5-11 Assumed saturation behavior of ΔE/E against time without cleaning or rain

This effect of dust represented by time, would be varied with the tilt angel of the PV and the average clearness index of the day.

From these assumptions a relation is assumed to calculate ΔE/E (the response) from the three factors discussed;

$$\frac{\Delta E}{E} = \frac{at}{b+t} \times (cK + d(\beta - \phi)) \qquad \text{(Eq. 5.4)}$$

Where a, b, c and d are all constants to be calculated using multiple nonlinear regression from the data obtained in the experiment.

$\frac{\Delta E}{E}$, is the (clean PV energy – the soiled PV energy)/ Energy of the clean PV

t, time in days since last time the soiled PV was cleaned or subjected to rain

K, is the average clearness index of the day

β, Is the tilt angle of the PV

ϕ, is the angle of latitude of the site where the PV is installed

K is calculated for every hour of sunlight and the daily average is then calculated. K is calculated as explained earlier in the chapter, using eq. 5.1. Thereby all variables are known and a multiple regression model is used to calculate the constants.

JMP pro software is used for this part of the analysis. First of all the data is organized in a table, ΔE/E in one column, time, β, K and ϕ each in a column. The tabulated data is inserted in a new JMP data file as shown in Fig (5-12);

File Edit Tables Rows Cols DOE Analyze Graph Tools View Window Help

Untitled 5

Columns (7/3)
- DeltaE/E
- beta
- K
- phi
- time
- formula
- FORMULA 2

Rows

	DeltaE/E	beta	K	phi	time
1	0.046520753	60	0.792539085	30	1
2	0.068462983	60	0.591490002	30	2
3	0.072732293	60	0.596683917	30	3
4	0.08276163	60	0.662418605	30	4
5	0.072079553	60	0.414109621	30	19
6	0.089211186	60	0.535707647	30	20
7	0.074581693	60	0.5025199	30	21
8	0.070289897	60	0.527484362	30	22
9	0.081018634	60	0.468467906	30	23
10	0.091934501	60	0.520598028	30	24
11	0.089126464	60	0.540864031	30	25
12	0.08251913	60	0.522221958	30	26
13	0.088148191	60	0.601929086	30	35
14	0.082243119	60	0.665456702	30	36
15	0.06806554	60	0.778272871	30	37
16	0.089383213	60	0.588286565	30	38
17	0.092801078	60	0.60260073	30	39
18	0.121969352	60	0.617245727	30	46
19	0.217192507	60	0.385532114	30	47
20	0.006392766	45	0.792539085	30	1
21	0.074245711	45	0.591490002	30	2
22	0.103727772	45	0.596683917	30	3
23	0.092146125	45	0.662418605	30	4
24	0.057887537	45	0.414109621	30	19
25	0.09776009	45	0.535707647	30	20
26	0.063613223	45	0.5025199	30	21
27	0.056541972	45	0.527484362	30	22
28	0.0880162	45	0.468467906	30	23
29	0.08130241	45	0.520598028	30	24
30	0.077564588	45	0.540864031	30	25

Figure 5-12 screenshot of JMP pro software, with the data from the experiment is inserted

After that the equation (Eq.5.4) is inserted in a new column, and the nonlinear modelling option is used where, ΔE/E is the response and the equation is the predicted from variables.

The result for this regression was,

a= -12.6465
b= 3.403879
c= -0.03691
d= 0.00043

Making the equation look like this,

$$\frac{\Delta E}{E} = \frac{-12.6465t}{3.403879+t} \times (-0.03691K + 0.00043(\beta - \phi)) \qquad \text{(Eq.5.5)}$$

$\frac{\Delta E}{E}$ Is calculated by this formula for the same data points used in the regression and then compared to the actual drop of energy. Fig (5-11) shows the predicted drop in energy (calculated by the formula) against the actual drop in energy measure during the experiment.

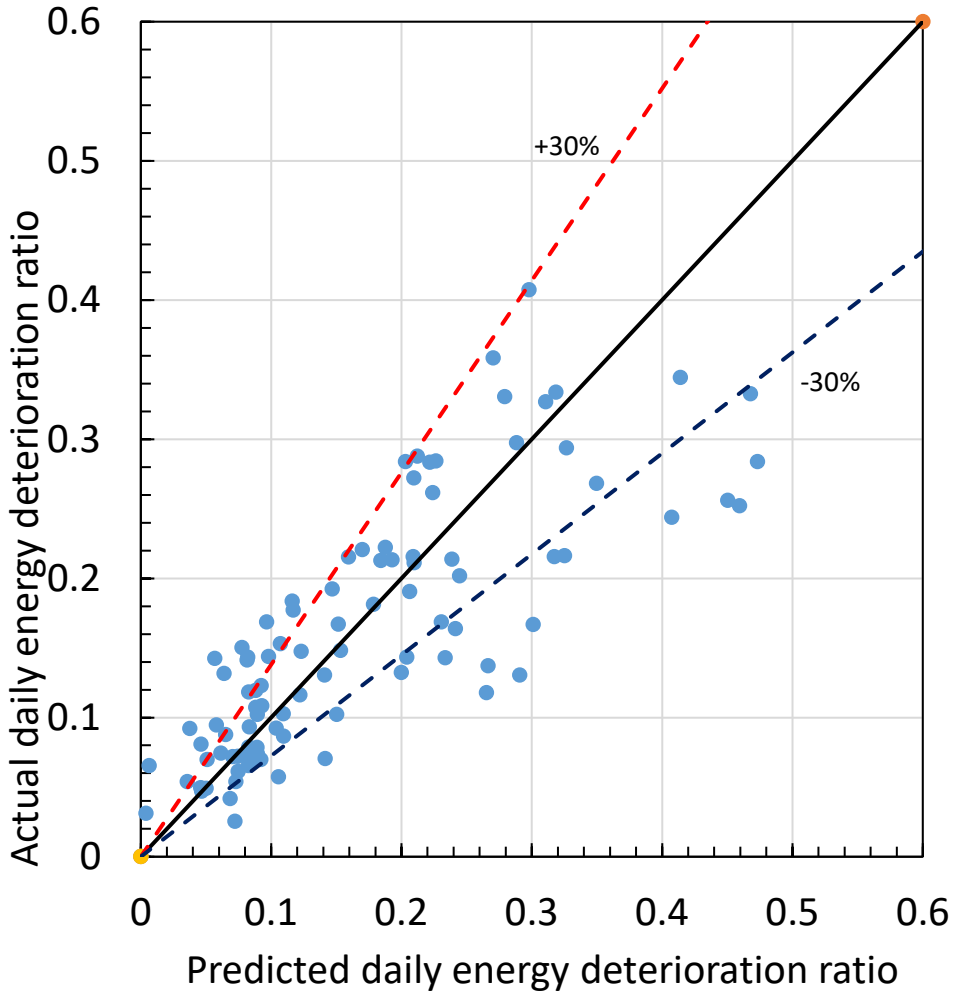

Figure 5-13 predicted energy drop against actual energy drop

As seen in figure (5-13) most of the points lie in the 30% range of the actual measured drop. The black line represent value of where the measured actual value is equal to the calculated or predicted value. The black and red dotted lines represent $\pm$30% of this value.

The coefficient of determination of this formula (r^2) is 0.6, and the correlation coefficient (r) is 0.78.

Thereby, this equation gives a pretty good estimate of total daily energy deterioration.

The same analysis is used to come up with an expression for the power drop between the clean and soiled PVs. The power drop within the day is a factor of the angle of incidence (θ) and the instantaneous clearness index (K), and time without cleaning or rain for the soiled PV, as discussed earlier in this chapter.

A power law regression model is assumed for this equation, and to simplify the regression model and minimize the K interactions, the readings are organized in terms of K and the formula is done for different K ranges, ranging from 0.2-0.8, each range with its unique constants.

The equation for the power drop is assumed to look as follows;

$$\frac{\Delta P}{Pclean} = At^{B}\frac{1}{(cos\theta)^{C}} \qquad \text{(Eq.5.6)}$$

Where,

$\frac{\Delta P}{Pclean}$, is ratio in power drop, (P clean-P soiled)/P clean

t is the time in minutes from last time PV was cleaned or subjected to rain

Cosθ, is cosine the angle of incidence

A, B & C are constants to be determined for different K ranges.

JMP pro is used in the same manner as the energy equation, but taking each readings of power, time and cosθ for the same K range separately.

For each k range A, B&C came out as follows,

Table 5-1 Regression equation constants for different K ranges

K	A	B	C
K=0.7-0.8	0.070652	0.000553	3.377628
K=0.6-0.7	0.005008	0.28333	2.791513
K=0.5-0.6	0.008636	0.235522	2.742466
K = 0.4-0.5	0.014950	0.215397	1.944965
K = 0.3-0.4	0.012755	0.229146	1.874622
K = 0.2-0.3	0.007189	0.267979	2.135077

Fig (5-14) shows the actual power drop against the predicted power drop using the formula for K range 0.5-0.6

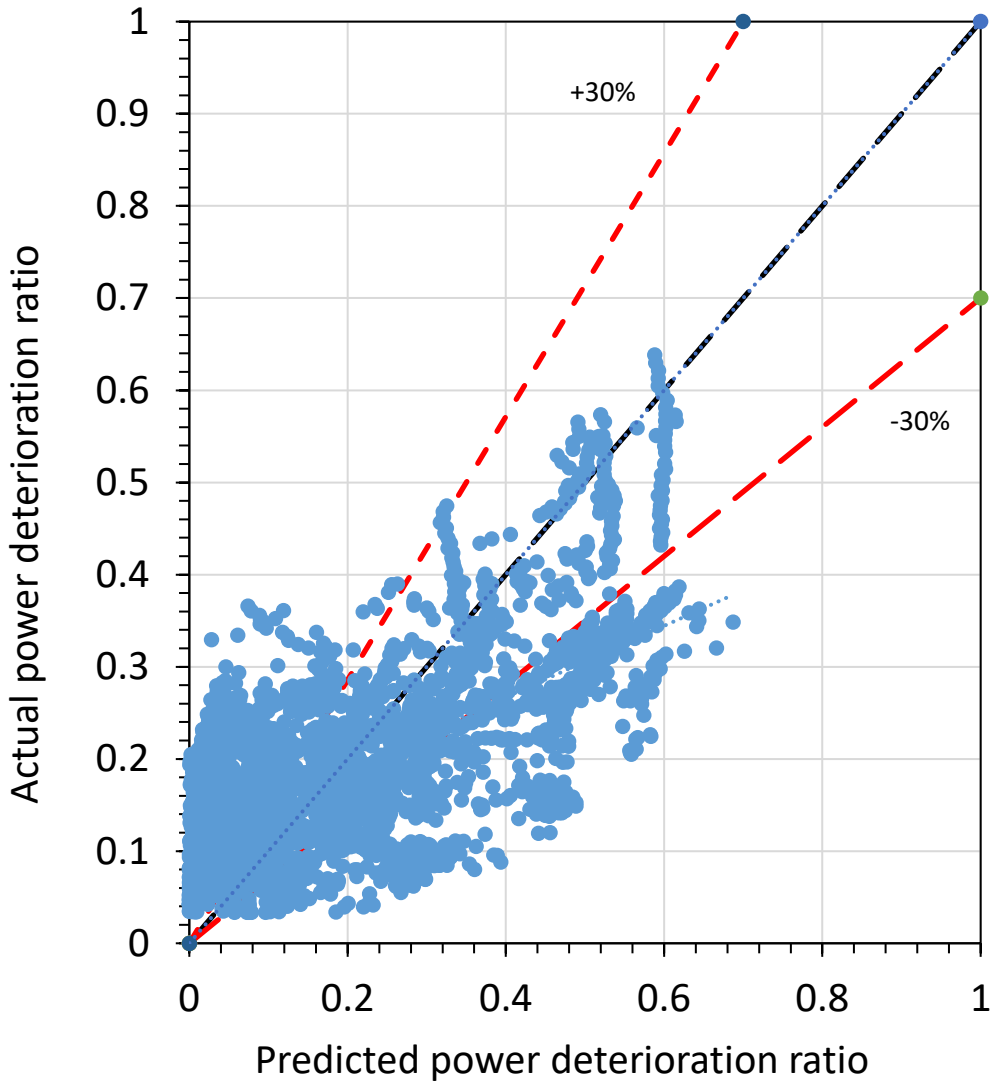

Figure 5-14 $\frac{\Delta P}{Pclean}$ actual against $\frac{\Delta P}{Pclean}$ predicted

The correlation coefficient (r) is 0.63 for this range of clearness index, K.

Chapter 6

6.1 Conclusion and recommendations

The aim of this research work was to investigate how different external factors affect the performance of PVs in working sites. The combined effect on a PV performance due to dust accumulation over the PVs tilt angle, the day's clearness index and the angle of incidence was investigated experimentally. From the three months study of the PVs at different tilt angles several conclusions were drawn.

i- Effect on Daily energy performance

Measurements revealed that lower tilt angles of PVs will produce more deterioration in performance. This is explained to be due to higher dust accumulation in less vertical PVs since the gravity component is weaker and hence less capable of detaching the dust particles from the glazing.

On the other hand, Rain cleans the surface of the PVs and restore them to their original performance, an example was the on 22nd of November after which the dirty PVs preformed as well as the clean PVs for several days.

The deterioration on the daily energy output after 2 months was as much as 20% for the PVs at tilt angle 60 and increased with lowering the tilt angle that it reached 40% drop with the unclean 15 degrees tilt angle PVs.

The magnitude of the impact of the dust depends on weather conditions, clear skies with strong solar radiation produce lower impact of the dust on performance, while unclear skies would heighten the impact of the dust on the performance. This effect is increased with lower tilt angles, as there is more dust accumulated. This was established in the experimental work as a direct relation with the clearness index of the day and this phenomena can be explained by that as the clearness index increase (clear sky) the percentage of the diffuse radiation decrease, and thus most of the radiation reaching the PVs would be beam radiation so a larger percent of that radiation penetrate the dust layer formed on the PVs and is utilized. On the other hand, when the clearness index is low (unclear sky) the diffuse radiation percentage is high , which is either reflected or refracted by the dust layer accumulated on the PV , thereby, amount of radiation utilized is low impacting the output of the PV.

ii- Instantaneous effect on power performance

Another factor that influence the effect of dust is the angle of incidence of the radiation , as the angle of incidence decreases (lowest at solar noon) when the radiation beams are almost vertical on the PVs the effect of dust is minimal , as most of the radiation penetrate the dust layer. While during early morning and afternoon the incidence angle increase thus the portion of solar radiation that is reflected increase. This is why all PVs clean and unclean have almost identical power outputs at the solar noon, and the effect of dust is at its highest at the early morning and in the afternoon.

For the PVs at tilt angle 60 after 30 days without cleaning, the power ratio of the soiled to the clean PV is increased at noon, and when the day is clear as in 18th of December it could reach 1, i.e. the soiled is producing the same power as the clean PV. But on the following day the solar radiation was fluctuating

and lower, implying lower clearness index, thereby at noon, the soiled PV produced substantially lower output than that of the clean PV.

This dust impact can be more severe than those percentages if the utilizabilty is taken into account, which is the useful power produced above a critical threshold. An example was discussed in the previous chapter where the utilizabilty of the clean PV dropped from 22% to just 2% due to the effect of dust accumulation or soiling.

iii- Regression models

Huge amounts of data were collected over the course of the 3 month experiment since measurements were recorded every 15 seconds. From these data, nonlinear regression models were derived to present the drop in daily energy output as well as instantaneous drop in power for different ranges of clearness indices. The derived energy drop regression equation is;

$$\frac{\Delta E}{E} = \frac{-12.6465t}{3.403879+t} \times (-0.03691K + 0.00043(\beta - \phi)) \qquad \text{(Eq.6.1)}$$

Where,

$\frac{\Delta E}{E}$, is the (clean PV energy – the soiled PV energy)/ Energy of the clean PV

T, time in days since last time the soiled PV was cleaned or subjected to rain

K, is the average clearness index of the day

β, Is the tilt angle of the PV

ϕ, is the angle of latitude of the site where the PV is installed

The correlation coefficient for this formula was r = 0.78 which is remarkably good, considering the large number of variables involved, their nonlinear interactions and the simplicity of the regression equation.

Then the best fit regression equation derived for the instantaneous power drop is;

$$\frac{\Delta P}{Pclean} = At^B \frac{1}{(cos\theta)^C} \qquad \text{(Eq.6.2)}$$

Where,

$\frac{\Delta P}{Pclean}$, is ratio in power drop, (P clean-P soiled)/P clean

t is the time in minutes from last time PV was cleaned or subjected to rain

Cosθ, is cosine the angle of incidence

A, B & C are constants to different for different K ranges.

However the correlation coefficient for these power equations are much poorer ranging from r = 0.45 to r = 0.63; this is traced to the high level of fluctuations in the measured power profiles. The exact cause of these fluctuations were not thoroughly investigated. However, it is believed to be due to the nonlinear interactions between the various variables, which was not expressed in the selected regression equation. In interest of simplicity a power law regression model was employed, however such model cannot capture those large fluctuations; although it follows the average trend quit faithfully. This may explain why the daily average energy regression equation present a much better fit.

An important question is what is the cause of these large fluctuations and the significance of their estimation. This issue requires further investigation.

It is remarked that the work conducted here was based on field measurements with all real life complications; thus the interactive effect of all variables affecting PV performance was present. Previous work was mainly conducted in controlled lab environment with fixed parameters, and single effects investigated; however as this work revealed that this has little relation to field performance.

6.2 Future work recommendations

The following recommendations are presented for further extension of the presented work:

1- Investigate the exact cause of the fluctuation of in the performance of the soiled PVs as pointed out. The conclusion based on these investigations may be used to derive a better regression equations, particularly for the instantaneous performance.
2- Extend the measurements to an entire year, while using larger recording intervals, since the 15 seconds intervals employed were unnecessary small, and requires complicated regression formulae to capture the variations.
3- Separate the effect of the tilt angle and the incidence angle
4- Combining the effect of the clearness index with the regression equation, rather than presenting different constants for different clearness indices ranges.

References

[1] B. K. Hodge, “Alternative Energy Systems,” John Wiley and Sons; April 2009.

[2] B.V. Chikate, Y.A. Sadawarte , ” The Factors Affecting the Performance of Solar Cell“ International Journal of Computer Applications (0975 – 8887) , International Conference on Quality Up-gradation in Engineering, Science and Technology 2015

[3] G. Makrides, B. Zinsser, M. Norton and G. E. Georghiou,”Performance of Photovoltaics under Actual Operating Conditions”

[4] M.S. El-Shobokshy, F.M.Hussein, “Effect of the dust with different physical Properties on the performance of photovoltaic cells.” Solar Energy 1993; 51(6):505–11.

[5] H. A Kazem et al. , T. Khatib, K. Sopian, F. Buttinger, W. Elmenreich, A. S. Albusaidi , “Effect of Dust Deposition on the Performance of Multi-Crystalline Photovoltaic Modules Based on Experimental Measurements” , INTERNATIONAL JOURNAL of RENEWABLE ENERGY RESEARCH, Vol.3, No.4, 2013

[6] D. Goossens, Z.Y Offer, A. Zangvil, “Wind tunnel experiments and field investigations of eolian dust deposition on photovoltaic solar collectors.” Solar Energy 1993; 50(1):75–84.

[7] M. Sow, D. Goossensa, and J.L. Rajot. “Calibration of the MDCO dust collector and of four versions of the inverted frisbee dust deposition sampler”, Geomorphology, Vol. 82, No. 3-4, 2006, pp. 360-375.

[8] AA. Hegazi, “Effect of dust accumulation on solar transmittance through glass covers of plate-type collectors.” Renew Energy 2001; 22:525–40.

[9] H.K. Elminir, A.E. Ghitas, R.H. Hamid, F. El-Hussainy , M.M. Beheary, K.M Abdel-Moneim, “Effect of dust on the transparent cover of solar collectors.” , Energy Convers Manage 2006; 47(18–19):3192–203.

[10] Z. AHMED, H. A. KAZEM and K. SOPIAN, “Effect of Dust on Photovoltaic Performance: Review and Research Status”

[11] N. S. Beattie, R.S. Moir, C. Chacko, G. Buffoni, S. H. Roberts, N. M. Pearsalla. “Understanding the effects of sand and dust accumulation on photovoltaic modules”, *Renewable Energy*, Vol. 48, 2012, pp. 448-452.

[12] J.K Kaldellis., P. Fragos. “Ash deposition impact on the energy performance of photovoltaic generators”, *Journal Cleaner Production*, Vol. 19, No. 4, 2011, pp. 311-317.

[13] A.A.M. Sayigh, S. Al-Jandal, H. Ahmed.” Dust effect on solar flat surfaces devices in Kuwait”,

Proc. of the Workshop on the Physics of Non- Conventional Energy Sources and Materials Science for Energy, Italy, 1985, pp. 353-367.

[14] J. A. Duffie, W. A. Beckman, “Solar Engineering of Thermal Processes”, Fourth Edition.

[15] Mosalam. H., Eldahan. O. H.,“Statistical analysis on the impact of Dusty Weather on Power Output of Solar Cells on Commercial Roof-top PV Systems in Egypt”

[16] J. R. Taylor,” Introduction to error analysis”, second edition, University Science Books, 1997

[17] JMP PRO 13 software, developed by SAS